Chronic fluoride poisoning during the Roman period in Cumae (Italy): a diagnostic approach to skeletal fluorosis in cremated human remains

Eliza Orellana-González, Sacha Kacki, Henri Duday, Yannick Lefrais, Priscilla Munzi, Rémy Chapoulie, Dominique Castex

BMSAP

Bulletins et mémoires de la société d'anthropologie de Paris
BMSAP

37 (1) | 2025
Varia

Chronic fluoride poisoning during the Roman period in Cumae (Italy): a diagnostic approach to skeletal fluorosis in cremated human remains

Intoxication chronique au fluor durant l'époque romaine à Cumes (Italie) : une approche diagnostique de la fluorose osseuse sur des restes humains brûlés

Eliza Orellana-González, Sacha Kacki, Henri Duday, Yannick Lefrais, Priscilla Munzi, Remy Chapoulie et Dominique Castex

OpenEdition Journals

Édition électronique
URL : https://journals.openedition.org/bmsap/15691
DOI : 10.4000/13pt5
ISSN : 1777-5469

Éditeur
Société d'Anthropologie de Paris

Référence électronique
Eliza Orellana-González, Sacha Kacki, Henri Duday, Yannick Lefrais, Priscilla Munzi, Remy Chapoulie et Dominique Castex, « Chronic fluoride poisoning during the Roman period in Cumae (Italy): a diagnostic approach to skeletal fluorosis in cremated human remains », *Bulletins et mémoires de la Société d'Anthropologie de Paris* [En ligne], 37 (1) | 2025, mis en ligne le 25 mars 2025, consulté le 01 mai 2025. URL : http://journals.openedition.org/bmsap/15691 ; DOI : https://doi.org/10.4000/13pt5

Chronic fluoride poisoning during the Roman period in Cumae (Italy): a diagnostic approach to skeletal fluorosis in cremated human remains

Intoxication chronique au fluor durant l'époque romaine à Cumes (Italie) : une approche diagnostique de la fluorose osseuse sur des restes humains brûlés

Eliza Orellana-González [1,2,3]*, Sacha Kacki [1,4], Henri Duday[1], Yannick Lefrais[2], Priscilla Munzi [5], Remy Chapoulie [2], Dominique Castex [1]

1 UMR 5199, PACEA, CNRS – Université de Bordeaux, Pessac, France
2 UMR 6034, Archéosciences Bordeaux, CNRS – Université Bordeaux Montaigne, Pessac, France
3 École française de Rome, Rome, Italy
4 Department of Archaeology, Durham University, Durham, United Kingdom
5 CNRS, Centre Jean Bérard, UAR 3133, CNRS-EFR, Naples, Italy

* eliza.orellana-gonzalez@u-bordeaux.fr

Reçu : 20 avril 2024 ; accepté : 06 novembre 2024
Bulletins et Mémoires de la Société d'Anthropologie de Paris

Abstract – Skeletal fluorosis is a pathological condition resulting from prolonged ingestion of large quantities of fluoride and causing increased bone formation and density. This disease is often endemic in volcanic areas where groundwater frequently contains high levels of fluoride. This study offers a multidisciplinary approach, combining palaeopathological observations and archaeometric analyses, for the diagnosis of skeletal fluorosis in human remains found in secondary cremation burials dating from the Roman period (2nd century BC – 1st century AD). The study sample is made up of 45 individuals from the ancient city of Cumae (Campania, southern Italy) in the volcanic region of the Phlegraean Fields. Pathological lesions were recorded using a macro-observation protocol. Fluoride detection and measurements were performed using Laser-induced breakdown spectroscopy (LIBS). The results confirm that the bones of these Cumae inhabitants had high fluoride concentrations and pathological lesions most likely related to bone fluorosis. 49% of the subjects in the study sample were classified into categories of moderate to high suspicion of fluorosis, indicating potential environmental poisoning probably linked to the volcanic nature of the region and the consumption of groundwater.

Keywords – endemic fluorosis, groundwater, historical ecotoxicology, paleopathology, LIBS, archaeometry

Résumé – La fluorose osseuse est une pathologie liée à l'ingestion prolongée de grandes quantités de fluorure, qui entraine notamment une augmentation de la densité des os. Cette maladie sévit souvent à l'état endémique dans certaines zones volcaniques où les eaux souterraines contiennent des doses élevées de fluor. Cette étude vise à proposer une approche multidisciplinaire combinant observations paléopathologiques et analyses archéométriques pour le diagnostic de la fluorose osseuse des restes humains provenant de sépultures secondaires à crémation de la période romaine (IIe siècle av. J.-C. – Ier siècle apr. J.-C.). L'échantillon étudié est composé de 45 individus originaires de la ville de Cumes (Campanie, sud de l'Italie), dans la région volcanique des Champs Phlégréens. Les lésions pathologiques ont été enregistrées selon un protocole d'observations macroscopiques. La détection et les mesures de fluor ont été effectuées par Spectroscopie d'émission atomique de plasma induit par laser (LIBS). Les résultats ont permis de confirmer que les os des habitants de Cumes présentaient des concentrations élevées de fluor et des lésions pathologiques très probablement liés à la fluorose osseuse. 49 % des sujets étudiés a été classé dans les catégories de suspicion modérée à forte de fluorose, indiquant une potentielle intoxication environnementale. Cela est probablement liée au caractère volcanique de la région et à la consommation des eaux souterraines.

Mots clés – fluorose endémique, eaux souterraines, écotoxicologie historique, paléopathologie, LIBS, archéométrie

Introduction

Fluoride, the ion-derived form of the element fluorine,[1] is an essential element for human health, and specifically for the formation of bones and teeth. Good health depends

1 Fluorine is the first element of the halogen group in the periodic table (atomic number 9, relative atomic mass 19). It rarely appears in the natural environment in its elemental form (Zohoori and Duckworth, 2017). Conversely, fluoride is abundant in the environment, taking on various forms as it combines with other elements (Barbier et al., 2010).

on a delicate balance of this element in the body: on the one hand, too little fluoride can lead to poor bone mineralisation and a high prevalence of dental caries. On the other hand, too much fluoride can result in pathological conditions such dental and skeletal fluorosis (WHO, 1992; 2019; Zohoori and Duckworth, 2017). The most frequent signs of dental fluorosis include developmental hypoplasia defects, staining, and surface irregularities in the enamel (Littleton, 1999). In contrast, skeletal fluorosis is a chronic metabolic bone disease that is caused by prolonged and excessive ingestion of fluoride. It affects a variety of cells involved in bone turnover, resulting in abnormal bone densification (Teotia et al., 1971; Boivin et al., 1989; Littleton, 1999; Petrone et al., 2013; Wei et al., 2019). Clinically, early symptoms can include stiffness and pain in the joints. Severe cases can be crippling and are associated with osteosclerosis, calcification of tendons and ligaments and bone deformities (Teotia et al., 1971; 1986; Teotia and Teotia, 1988; Boivin et al., 1989; Littleton, 1999; Petrone et al., 2013; Nelson, 2015; Nelson et al., 2016; 2019; Zohoori and Duckworth, 2017; Zuo et al., 2018; Wei et al., 2019; WHO, 2019; Walser et al., 2020). The condition also causes extensive sub-periosteal and endosteal bony accretion, often accompanied by increased resorption of the old cortex on the long bones, making the bones weaker than normal and increasing the risk of fractures (Ortner, 2003; Brickley and Ives, 2008b; Petrone et al., 2013; Nelson et al., 2016). The condition is cumulative and gradual (WHO, 2019), and the pathological bone modifications it causes may decrease overall life expectancy (Walser et al., 2020). Prolonged fluoride intake (exceeding ten years) can lead to mild skeletal changes, with fluoride accumulation slowing and reaching a plateau after approximately 55 years of age (Ayoob and Gupta, 2006; Ponikvar, 2008). If fluoride intake ceases, the reduction of fluoride levels in bone occurs gradually (Khairnar et al., 2015). However, there are still few published data on the relationship between bone fluoride levels, age and fluoride concentrations in water.

In the environment, fluoride is naturally present in soils, water, air and dust. It can also be present as a result of human activities such as industrial pollution (*e.g.* aluminium industry) or as an artificial additive in foodstuffs, water or dental care products (WHO, 1992; Ayoob and Gupta, 2006; Ghosh et al., 2013; Zohoori and Duckworth, 2017). Despite this wide variety of sources, water is considered to be the main source of fluoride, with concentrations varying between geographic regions and influenced by parameters such as pH, temperature and water hardness (WHO, 1984; Ayoob and Gupta, 2006; Barbier et al., 2010; Zohoori and Duckworth, 2017; Chowdhury et al., 2019). Groundwater in volcanic regions is particularly rich in fluoride. Hydrogen fluoride is one of the most soluble gases in magma, and is partially released into the environment during eruptive activity. It is also released with fumarole gases and by degassing from volcanic systems, then dissolving when it comes into contact with water (D'Alessandro, 2006; Yeşilnacar et al., 2016; Sahu, 2019). As a consequence, while fluoride concentrations in unpolluted surface waters are usually between 0.01-0.3 mg/l, groundwater in volcanic areas and in areas with geological deposits of marine origin usually contain high fluoride concentrations, up to 30-50 mg/l (Barbier et al., 2010; Shamsollahi et al., 2015; Zohoori and Duckworth, 2017). These figures are higher than World Health Organization (WHO) recommendations for fluoride intake in drinking water, which should not exceed 1.5 mg/l, because higher doses could lead to poisoning (WHO, 1992; 2019).

In modern times, high levels of fluoride in groundwater, and the resulting fluorosis, have been raising significant environmental and public health challenges (Ghosh et al., 2013; WHO, 2019; Srivastava and Flora, 2020; Shaji et al., 2024). Skeletal fluorosis affects millions of people worldwide and is prevalent in many volcanic areas (WHO, 1992; D'Alessandro, 2006; Barbier et al., 2010), particularly those associated with the five fluoride belts. These belts include, for example, Turkey and the East African Rift in Belt 1; Northern Africa in Belt 2; India, Iran, Iraq, and China in Belt 3; Southern Europe, the United States, and Latin America in Belt 4; Japan and Indonesia in Belt 5 (for more information see Chowdhury et al., 2019).

As for past populations, a few studies have demonstrated the presence of skeletal fluorosis in different geographic regions and in a variety of chrono-cultural and geological contexts, including areas of volcanic activity (Callaghan, 1986; Littleton, 1999; Weinstein, 2005; Yoshimura et al., 2006; Nelson, 2015; Nelson et al., 2016; 2019; Walser et al., 2020; Zhou et al., 2023). It should be noted, however, that these studies have mainly focused on non-cremated skeletal remains. As a result, no proper protocol has been proposed to diagnose the condition in cremated human remains, although they are the main source of data for some chrono-geographical contexts (notably in southern Europe during a large part of the Roman period until the end of the 2nd century AD).

Our study addresses this issue by investigating the possible evidence of fluoride poisoning in the Campanian region of southern Italy during the Roman period (2nd century BC – 1st century AD) through palaeopathological observations and chemical analyses of osteological remains from secondary cremation burials.[2] Even though Italy is often not considered to be part of the above-mentioned fluoride belts, there is modern evidence of endemic fluorosis in southern locations, such as Sicily (D'Alessandro, 2006) and Naples (Eager, 1901; Petrone et al., 2013). Moreover, ancient cases

2 A "secondary cremation burial" should be understood as follows: "*a cremation burial is considered to be secondary when a corpse is burnt on a pyre. Its flesh disappears while the bones are collected and preserved in a vessel that can be buried at some distance from the pyre*" (Duday, 2009:90). The manipulation of burnt bones as a funerary gesture immediately after burning the corpse is pre-planned and should be distinguished from other funerary practices that involve burning loose bones and then depositing them elsewhere.

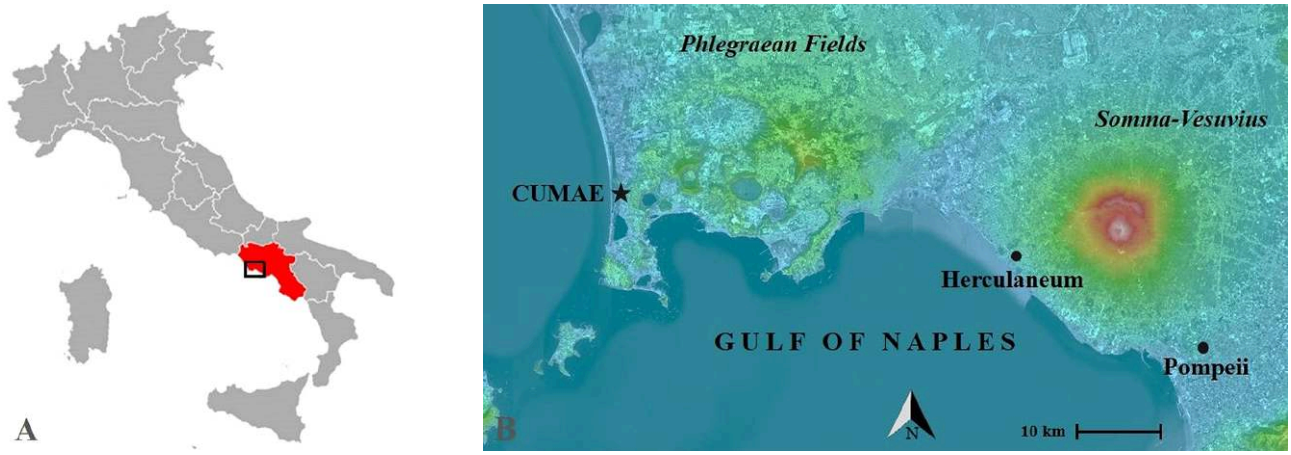

Figure 1. A) Map of Italy highlighting the Campanian region, where Cumae is located; B) Cumae, shown by a star, is situated amidst the volcanic area of the Phlegraean Fields to the north of the Gulf of Naples; to the south, Herculaneum and Pompeii are situated within the Somma-Vesuvius volcanic area (adapted from https://tessadem.com/) / *A) Carte de l'Italie mettant en évidence la région de Campanie, où se trouve Cumes; B) Au nord du golfe de Naples, Cumes, représentée par une étoile, est située au sein de la zone volcanique des Champs Phlégréens; Herculanum et Pompéi, au sud, sont situés dans la zone volcanique de Somma-Vésuve (modifié d'après https://tessadem.com/)*

of fluorosis have already been identified in buried human remains in this region, both in the Somma-Vesuvius area at Herculaneum (Torino et al., 1995; Petrone et al., 2011; 2013; 2019) and at the site of Cumae in the Phlegraean Fields (Torino et al., 2012) (see the locations of the cited sites in figure 1). Recently, a few researchers have highlighted the possible presence of the condition in cremated remains preserved in the necropolis of Porta Nocera in Pompeii (Van Andringa et al., 2013; 2021) and the Necropolis of Porta Mediana at Cumae (Duday, 2018; 2019), mainly based on observations of increased bone density in the remains of single burials. This study aims to examine this hypothesis for the second of these sites and to develop a detailed protocol to assess the presence of skeletal fluorosis in cremated human remains.

Materials

Cumae: geological formation and history of the site

The Cumae archaeological site is located in the Phlegraean Fields, a volcanic region to the west of Naples in southern Italy (figure 1). Numerous eruptions have occurred over the history of this super-volcano, which is still active. These eruptive events have caused the formation of mostly single-edifice structures and the deposition of significant amounts of pyroclastic rocks along with occasional small-scale lava flows. Researchers have divided its volcanic activity into a pre-calderic period[3] (ca. 80 to 60 Ky) characterised by the formation of multiple separate volcanic centres followed by two major volcanic events: the Campanian Ignimbrite eruption (39 Ky BP) and the Neapolitan Yellow Tuff (15 Ky BP). Contrary to the Somma-Vesuvio, also located in the Campanian volcanic arc, the eruptive activity of the Phlegraean Fields is spread over a very large area, in which numerous small volcanic systems have formed (Rosi et al., 1983; Bousquet, 2018; Forni et al., 2018; Stellato et al., 2020; Sbrana et al., 2021; Cappelletti et al., 2022). The Phlegraean Fields caldera also presents a unique phenomenon known as bradyseism, involving periodic vertical ground deformations over the centuries that have varied in scale from millimetres to metres. Explosive activity in this region is also characterised by water/magma interactions within a vast hydrothermal system (Adinolfi, 1978; Rosi et al., 1983; Di Vito et al., 1999; Orsi et al., 1999; Ciaramella et al., 2011; Calò and Tramelli, 2018). Due to this significant volcanic activity, the groundwater in the Phlegraean Fields is likely to contain elevated levels of fluoride, raising potential risks for both the environment and human health.

Historically, Cumae is one of the oldest Magna Graecia settlements around the Western Mediterranean Sea. The site has seen more than 20 centuries of human occupation, from indigenous occupations during the Bronze Age, followed by the Greeks' foundation in 740 BC and through to the abandon of the site between the 13th and 14th century AD. Around the second half of the 4th century BC, the Romans took control of the Campanian coasts. Cumae was then incorporated into Roman territory (*civitas sine suffragio*) and gained municipal status towards the end of the 1st century BC (Caputo et al., 1996; Munzi and Brun, 2011). Cumae's boundaries are marked by a partially defined wall circuit, encompassing Monte di Cuma on the north-western side and Monte Grillo on the eastern side (Caputo et al., 1996; Munzi and Brun, 2011).

3 The pre-calderic period is defined as a phase of submarine volcanism, with less frequent eruptions involving highly evolved, water-rich and relatively cold magma (Rosi et al., 1983; Forni et al., 2018; Sbrana et al., 2021).

Figure 2. Tomb ENF34009, a small "*a dado*" funerary monument from the Augustan age, and an urn containing cremated remains CU34242 (photographs: CJB archives) / *Tombe ENF34009, petit monument funéraire "a dado" d'époque augustéenne et sépulture secondaire à crémation CU34242 (clichés : archives CJB)*

The "Porta Mediana" necropolis, investigated by the Centre Jean Bérard since 2001, is located to the north-east of Monte di Cuma, just outside one of the northern city gates, also called the Porta Mediana. The excavations have revealed funerary practices attributed to different groups including Cumaeans, Greeks, Italics and Romans, thus confirming the continuous funerary function of this area from the period of indigenous settlements and the Greek colony until the early Middle Ages. The typology of the tomb architecture and the sepulchral characteristics display differences based on the chronology, cultures and religious beliefs of the communities that inhabited the settlement (Brun and Munzi, 2009; Munzi and Brun, 2011; Munzi, 2022).

By the second half of the 2nd century BC and the final years of the Republic, hypogean monuments marking the burial places of Cumae elites were mainly surrounded by secondary cremation burials of lower-class individuals,[4] arranged in multiple rows along roadsides. With the beginning of the Augustan age, mausoleums for the upper classes persisted while "*cippo*" tombs were gradually replaced by small "*a dado*" monuments with an aedicule façade and an underground funerary chamber (figure 2). The secondary cremation burials preserved in these monuments are mostly those of employees or freedmen of notable Cumae families. After the Augustan period, both cremation and inhumation continued, the former being slightly more prevalent. Most tombs built during the 1st century AD were columbaria intended to contain cremated remains in urns inserted into the walls. It was only after the 1st century AD that inhumation became the main funerary practice, in monuments as well as individual graves (Brun and Munzi, 2009; Brun et al., 2010; 2013; Munzi and Brun, 2011; Munzi et al., 2018; Munzi, 2022).

4 Between the 2nd and 1st centuries BC, secondary cremation burials were deposited either in parallelepiped tombs with a stele, or in pit tombs with a stone marker (*cippo*). They were consistently deposited in ceramic urns. The epitaph on the stone markers was most likely engraved or painted with the name of the deceased (Munzi, 2022).

The Cumae sample

This study covers forty-five individual burials of cremated remains in the Necropolis of Porta Mediana at Cumae. Only adults (*n*=43) and older adolescents (*n*=2) were included in our sample (table 1), as the completion of development and ossification makes bones less porous and fluoride uptake therefore proceeds at a more regular pace than in children (Teotia and Teotia, 1988; Whitford, 1994; 1999; Ozsvath, 2009). All these cremated remains were placed in sealed ceramic urns. Previous chemical analyses conducted by Loeff (2018) on a sample from Cumae, which included pottery fragments of the urn, its cover, and the plaster used to seal the funerary urn, found no traces of fluoride in these components of the funerary structure. These findings rule out the possibility of post-depositional contamination of the cremated remains inside the urns.

Sex and age assessment was conducted previously by one of the authors of this study (HD). Sex estimation was based on sexually dimorphic traits of the os coxae, following Bruzek (2002). To aid sex estimation, information from epitaphs was also used when available. The sex distribution of our sample was determined from these two criteria, resulting in 31% male individuals (*n*=14), 4% probably male (*n*=2), 47% female (*n*=21), 9% probably female (*n*=4), and 9% of indeterminate sex (*n*=4). Age estimation was based on the stage of bone maturation and development of the teeth, when these observations were possible. For the juveniles (between 16 and 20, *n*=2), age was estimated according to observations of secondary ossification centres, following Scheuer and Black (2000). For the adults, age was estimated on the basis of age-related changes to the auricular surface, following Meindl and Lovejoy (1989). Adults were classified into three age groups: young adults (20-29 years) (*n*=11), middle-aged adults (30-59 years) (*n*=23), and elderly adults (> 60 years) (*n*=9) (figure 3).

The palaeopathological observations involved a thorough study of all the remains from each individual. Following the recommendations of Turkekul and colleagues (2020),

Sample ID	Sample group	Treatment / Origin	Chronology	Sex estimation			Group of age	Cremation total weight	Analysis (Macro./LIBS)
				Coxae morphology	Epitaph	Final*			
CU2001	Cumae	B / V	15 BC-14 AD	F?	F	F	oA	1296.9	M/L
CU29008			100-75 BC	F?	-	F?	yA	1072.3	
CU29014			100-75 BC	F	F	F	oA	749.3	
CU29050			150-101 BC	M	-	M	oA	3627.6	
CU29060			100-75 BC	F	F	F	yA	1059	
CU34174			-	M?	-	M?	oA	1044.6	
CU34220			50-20 BC	M	M	M	mA	2260.9	
CU34241			1-50 AD	F	-	F	J	1847.2	
CU34242			30-1 BC	F	F	F	mA	1719.1	
CU34247			100-1 BC	F	-	F	oA	866.9	
CU34276			1-50 AD	M	-	M	mA	2200.3	
CU34279			1-50 AD	F	-	F	mA	1022.8	
CU34283			30-1 BC	F	F	F	mA	2220.9	
CU34243			1-50 AD	M	-	M	mA	4566.7	
CU34253			1-50 AD	M?	-	M?	mA	2651.1	
CU35335			15 BC-14 AD	F	-	F	yA	1059.3	
CU35370			25 -1 BC	M	-	M	yA	1970.5	
CU35381			25 -1 BC	F	-	F	yA	1389.1	
CU35383_35415			80-50 BC	Ind	F	F	mA	626.7	
CU35384			100-50 BC	F	-	F	mA	569.5	
CU35389			25 -1 BC	Ind	-	Ind	J	917.6	
CU35398			25 -1 BC	F?	-	F?	oA	342.6	
CU35410			25 -1 BC	F	-	F	yA	1361.2	
CU35414			50-1 BC	F	-	F	yA	1253.4	
CU35417			15 BC-14 AD	M	-	M	mA	3739.6	
CU35429			-	Ind	-	Ind	mA	550.2	
CU35482			100-75 BC	Ind	F	F	mA	1313.2	
CU35456			50-1 BC	M	-	M	mA	1711.1	
CU35461			50-1 BC	F	-	F	oA	1039.5	
CU35478			125-101 BC	M	-	M	mA	1446.5	
CU35490			125-75 BC	M	-	M	mA	847.3	
CU37043			50-1 BC	M	M	M	yA	1814.1	
CU37044			50-1 BC	M	M	M	mA	3055	
CU37045			40-1 BC	F	F	F	oA	965.6	
CU39392			100-75 BC	Ind	-	Ind	mA	361.2	
CU39186			100-75 BC	Ind	-	Ind	yA	229.1	
CU39305			75-50 BC	M	-	M	mA	2159.3	
CU39306			50-100 AD	M	-	M	mA	3547.5	
CU39353			75-25 BC	F	-	F	mA	333.8	
CU39381			100-75 BC	M	-	M	mA	909.5	
CU39389			50-100 AD	F	-	F	yA	1657.5	
CU39390			50-100 AD	F?	-	F?	oA	1331.8	
CU39391			50-100 AD	F	-	F	mA	1794.4	
CU39396			50-100 AD	F?	-	F?	mA	1936.8	
CU39397			25-50 BC	F	-	F	yA	1754.2	
RAC107US786R3	Control	B/nV	30 BC-14 AD	-	-	-	A	-	L
RAC173US865R1									
LCM84D14R3_femur		Ub/nV	Neolithic-Chalcolithic						
LCM84E14									
LCM84E15R5									

Table 1. Sample information and types of analyses undertaken. Legend: Treatment (funerary treatment): B = burnt, Ub = unburnt. Origin: V = volcanic area, nV = non volcanic area. Sex estimation: Ind = indeterminate, F = female, F? = Probably female, M = male, M? = probably male, - = not identified. Final* = Sex estimation after taking the two criteria into consideration (coxae morphology + epitaph). Group of age: J = juvenile (16-20 years), yA = young adult (20-29 years), mA = middle-aged adult (30-59 years), oA = elderly adult (> 60 years), A = adult (when no further detail was available). Analysis: Macro. = macroscopic analysis (palaeopathological protocol), LIBS = Laser-induced breakdown spectroscopy / *Information de l'échantillon étudié et les types d'analyses entreprises. Légende : Traitement (traitement funéraire) : B = brûlé, Ub = non brûlé. Origine : V = zone volcanique, nV = zone non volcanique. Diagnose sexuelle : Ind= indéterminé, F = féminin, F? = féminin probable, M = masculin, M? = masculin probable, - = non identifié. Final* = Diagnose sexuelle après prise en compte deux critères (morphologie coxale + épitaphe). Classe d'âge : J = juvénile (16-20 ans), yA = jeune adulte (20-29 ans), mA = adulte moyen (30-59 ans), oA = adulte âgé (> 60 ans), A = adulte (lorsqu'il n'était pas possible de donner une meilleure précision). Analyse : Macro. = analyse macroscopique (protocole paléo-pathologique), LIBS = Spectroscopie d'émission atomique de plasma induit par laser*

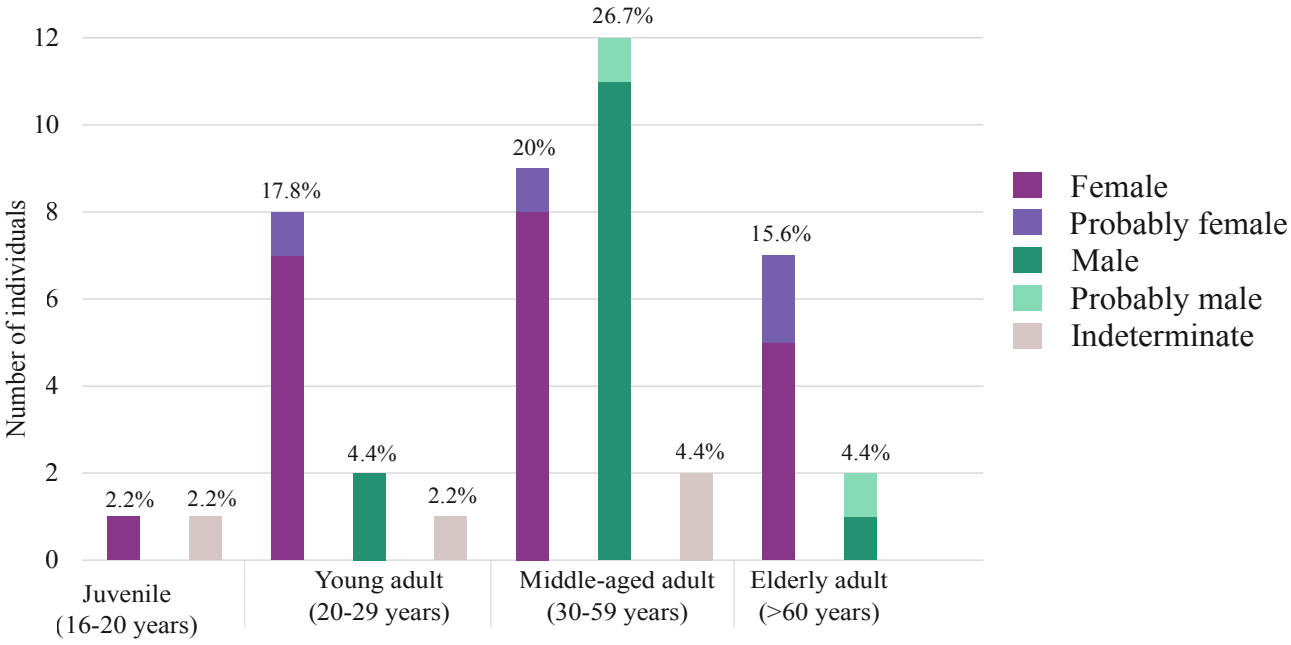

Figure 3. Demography of the Cumae sample. For each age group, sex estimation is specified along with the percentage relative to the whole sample (*n*=45) / *Démographie de l'échantillon de Cumes. Pour chaque classe d'âge, la diagnose sexuelle est précisée ainsi que le pourcentage par rapport à l'échantillon complet (n=45)*

a femur fragment was selected from each individual for archaeometric analysis. Preference was given to fragments from the femur's proximal third, particularly those containing the gluteal tuberosity when possible.

Control sample

In order to better assess fluoride enrichment in the Cumae sample, a control sample of six individuals from non-volcanic contexts was also analysed (table 1). Four of the samples were from a collective inhumation assemblage from the osteological Neolithic-Chalcolithic collection of La Caouno (Moux, Aude, southern France) (Gutherz, 1986). The other two individuals are cremated remains from an Augustan Roman necropolis at Classe (Ravenna, northeast Italy) (Scheid, 2008). These samples enabled us to assess whether there is a relevant difference in fluoride, firstly between volcanic and non-volcanic contexts, and secondly between non-cremated and cremated remains. Additionally, the comparison between the Cumae sample and the control sample provided a better understanding of variations in fluoride concentrations within the Cumae sample.

Methods

Palaeopathological observations: setting up a protocol for skeletal fluorosis

Previous research (Duday 2018; 2019) revealed the possible presence of skeletal fluorosis in cremated individuals from the Cumae sample, and highlighted the need to build up a specific protocol for this kind of material. The approach proposed in this research is based on skeletal fluorosis lesions documented in previous palaeopathological studies (Littleton, 1999; Brickley and Ives, 2008a; Petrone et al., 2011; 2013; Nelson et al., 2016; 2019; Walser et al., 2020; Zhou et al., 2023) and modern cases reported in the clinical literature (Jolly et al., 1968; Teotia et al., 1971; Teotia and Teotia, 1988; Buchancová et al., 2008; Qin et al., 2009; Izuora et al., 2011; Gupta and Ayoob, 2016; Kurdi, 2016; Zuo et al., 2018; Fabreau et al., 2019; Guan et al., 2019; Cook et al., 2021; Joseph et al., 2022). Our protocol takes into account the most frequent of these pathological bone changes, all of which can also result from other pathological conditions (table 2).

Pathological lesions were observed macroscopically in 12 different anatomical areas (figure 4): the cranial vault, vertebrae, ribs, sternum, glenohumeral joint, elbow joint,[5] wrist,[6] pelvic girdle, femur, patella, tibia and calcaneus. Teeth were excluded from our analysis since they are frequently broken and enamel tends to shatter due to the high temperatures and rapid desiccation that occur during cremation. Each of the regions considered can show one or more types of bone lesions (table 2). Each lesion was

5 Including the trochlear surface and capitulum of the humerus, the head of the radius, the trochlear notch and radial notch of the ulna.

6 Including the distal articular surface and ulna notch of the radius, and the radial circumferential articulation of the ulna.

Pathological feature		Possible differential diagnoses									
Bone	**Lesion or pathology**	***Osteoarthritis***	***DISH***	***Ankylosing Spondylitis***	***Myositis ossificans***	***Paget's disease***	***Hypoparathyroid***	***Osteopetrosis***	***Treponemal infection***	***Hematogenous Osteomyelitis***	***Skeletal fluorosis***
Cranial Vault	thickness increase - osteosclerosis				✓	✓	✓	✓			✓
Vertebrae	osteophytes, enthesophytes	✓	✓	✓	✓	✓	✓	✓	✓	✓	✓
	vertebral ankylosis			✓				✓	✓		✓
Ribs	widening and irregular edges				✓	✓	✓	✓			✓
	coarse porosity										✓
Sternum	cartilage ossification										✓
Scapula, Humerus, Radius, Ulna, Os Coxae, Femur, Patella, Tibia, Calcaneus	osteophytes	✓	✓	✓		✓	?	✓	✓	?	✓
	enthesophytes		✓	✓	✓						✓
	joint ankylosis			✓				✓	✓		✓
	periosteal reaction			✓			✓	?	✓	✓	✓
	fractures		✓		?	✓	?	✓			✓
Other Characteristics	mainly elderly individuals	✓	✓			✓					✓
	mainly men		✓	✓		✓				✓	✓
	bilateral or systemic	✓	✓			✓		✓	✓		✓
	mainly lower limbs						✓	✓		✓	✓
	abnormally heavy/thick bones				✓	✓	✓	✓	✓	✓	✓

✓ = present; ? = insufficient clinical information available / *✓ = présent ; ? = Données cliniques disponibles insuffisantes*

Table 2. Differential diagnoses of pathological signs analysed for this study (modified from Nelson 2015 and Nelson et al. 2016; 2019) / *Diagnostic différentiel des signes pathologiques analysés pour cette recherche (modifié d'après Nelson 2015 et Nelson et al. 2016 ; 2019)*

recorded as "present", "absent" or "non-observable". Given the fragmented and incomplete nature of cremated remains, at least 50% of the joint area or ligament insertion needed to be visible, even if spread across multiple fragments, in order to meet the criteria for observability.

We examined the cranial vault for indications of osteosclerosis and increased thickness, particularly on the frontal, parietal, and occipital bones. The presence of osteophytes and enthesophytes on the vertebrae was documented based on large anatomical regions (cervical, thoracic and lumbar). In addition to observing widening and irregular edges on the ribs, we considered coarse, diffuse porosity of the rib surface as possibly indicative of the mixed osteoblastic/osteoclastic activity associated with the disease. Another criterion added to our protocol was the presence of cartilage ossification on the sternum. Furthermore, ossification or calcifications in limb anatomical areas were noted in terms of presence or absence according to Villotte's classification of entheseal changes (Villotte et al., 2010; 2016; Villotte and Knüsel, 2013). Additionally, we documented fractures as well as bone lesions that are indicative of other conditions, such as Diffuse Idiopathic Skeletal Hyperostosis (DISH).

Because none of the pathological lesions recorded are pathognomonic of fluorosis, individuals were classified into three levels of suspicion for fluorosis, based on the percentage of observable anatomical areas showing bone changes across the twelve regions considered. "Strong suspicion" was assigned when more than 70% of preserved anatomical areas had lesions. "Moderate suspicion" encompassed cases where 30 to 70% of preserved anatomical areas had lesions. When less than 30% of the preserved anatomical areas showed lesions, the individual was recorded as having "no suspicion" of fluorosis. Our sample consisted mainly of fragmented and incomplete burnt remains that limited observations in many areas. To avoid extremely positive or negative diagnoses resulting from preservation biases, a category of fluorosis suspicion was assigned only when at least five anatomical regions could be observed. Thus, individuals with only four or fewer observable anatomical zones were classified as "non-attributable".

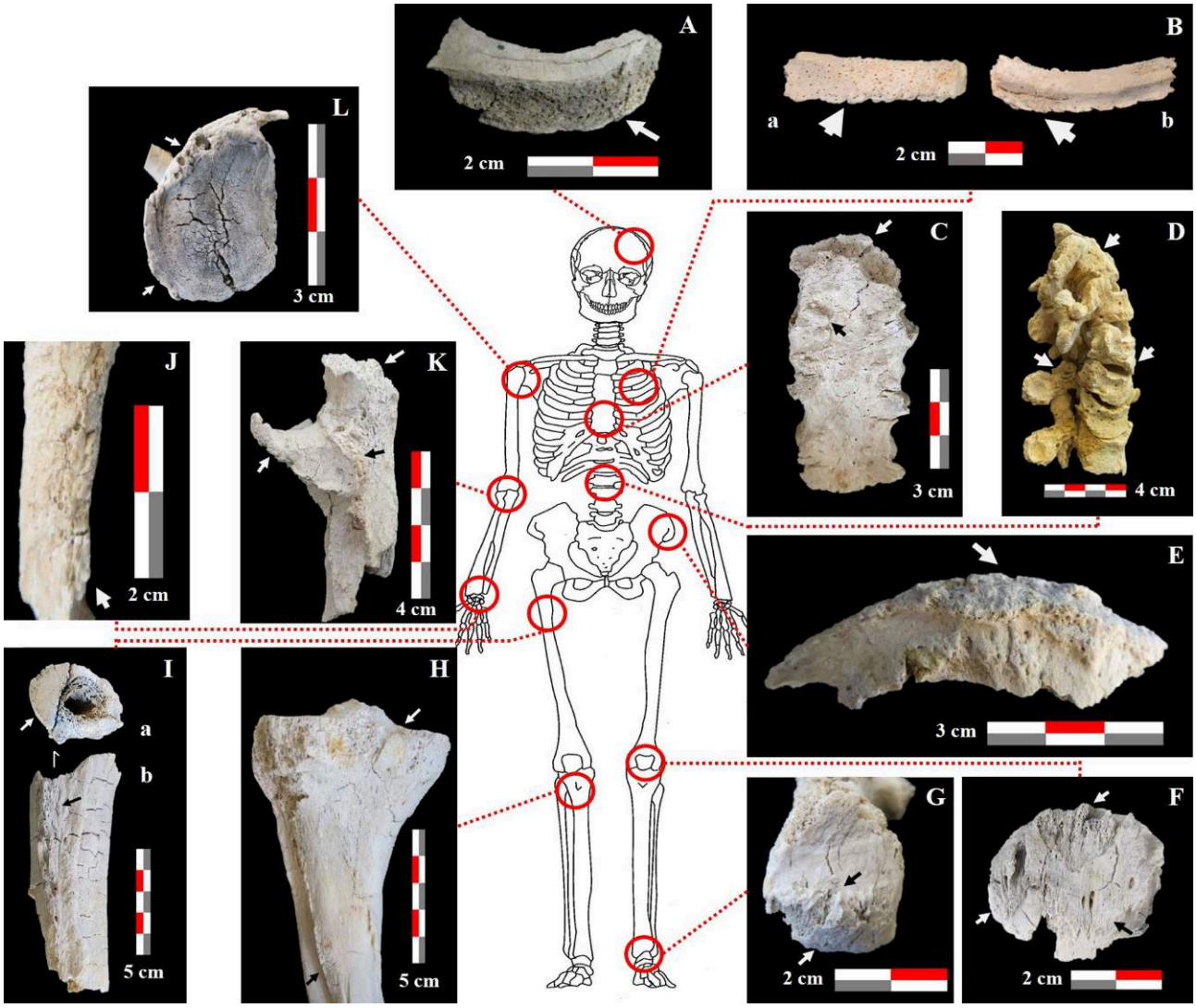

Figure 4. Anatomical zones considered in our protocol and examples of bone lesions observed in the Cumae sample. Arrows indicate bone modifications. A) Cranial vault fragment from CU34283; detail showing abnormal diploe thickness; B) Rib fragment from CU37044 exhibiting excessive bone formation, ossification of intercostal muscles on the superior and inferior margins, and porous surface alteration (a: exothoracic side, b: endothoracic side); C) Sternum fragment from CU39306 displaying cartilage ossification, particularly in the visceral surface and the articular facets; D) Cervicothoracic portion of the spinal column from CU37044 illustrating osteophytic development and excessive cartilage ossification on the articular processes; E) Iliac crest fragment from CU34220 with enthesophyte formation; F) Patella from CU34220 showing enthesophyte development; G) Calcaneal tuberosity from CU2001 displays enthesophyte formation and bony spicules; H) Posterior view of tibia fragment from CU37044 showing enthesophyte development on the soleal line; I) Femur fragment portion showing the *linea aspera* from CU37044 with excessive dense cortical development (a: section view, b: posterior view); J) Distal portion of radius fragment from CU35417 showing evidence of enthesophyte formation; K) Ulna fragment from CU29050 with enthesophyte growth on the trochlear notch; L) Glenoid fossa of scapula fragment from CU34220 with enthesophyte formation / *Zones anatomiques considérées dans notre protocole et exemples de lésions osseuses observées dans l'échantillon de Cumes. Les flèches indiquent les modifications osseuses. A) Fragment de voûte crânienne provenant du CU34283, le détail montre un épaississement anormal du diploë ; B) Fragment de côte du CU37044 avec formation osseuse excessive, ossification des muscles intercostaux sur les bords supérieur et inférieur et altération de la surface sous la forme de porosité (a : côté exothoracique, b : côté endothoracique) ; C) Fragment de sternum du CU39306 avec ossification du cartilage visible au niveau de la surface viscérale et des facettes articulaires ; D) Portion cervicothoracique de la colonne vertébrale du CU37044 illustrant le développement ostéophytique et l'ossification excessive du cartilage sur les processus articulaires ; E) Fragment de crête iliaque du CU34220 avec formation d'enthésophytes ; F) Patella du CU34220 montrant le développement d'enthésophytes ; G) Tubérosité calcanéenne du CU2001 présente la formation d'enthésophytes et de spicules osseux ; H) Vue postérieure d'un fragment de tibia du CU37044 montrant le développement d'enthésophytes sur la crête soléaire ; I) Fragment de fémur montrant la ligne âpre du CU37044 notamment l'épaisseur excessive de la corticale (a : vue en coupe, b : vue postérieure) ; J) Partie distale du fragment de radius du CU35417 avec la formation d'enthésophytes ; K) Fragment d'ulna du CU29050 avec formation d'enthésophytes sur l'incisure trochléaire ; L) Cavité glénoïdale du fragment de scapula du CU34220 avec formation d'enthésophytes*

Assessment of total weight and trunk weight index

As well as biological characteristics, total weight and weight index were also considered as pointers to suspected fluorosis, since values exceeding the theoretical weight for a single individual can be related to pathological processes on the skeleton (Van Andringa et al., 2013; Duday, 2018; 2019). McKinley's (1993) research on modern crematoria aimed to establish comparisons with archaeological cremations. The results show a total average weight for individuals of adult size of 1,627.2 g (σ=426.4 g) (male individuals: $\bar{x}$=1,864 g, σ=333.5 g; female individuals: $\bar{x}$=1,271.9 g, σ=280.7 g). Despite the differences, there is a substantial overlap between the sexes, also demonstrated by other studies (see Duday et al., 2000:8). Moreover, there seem to be differences between modern and archaeological data that can be attributed to several factors. Most archaeological remains studied are from secondary cremation burials, often with no complete skeleton. Additionally, sediment in the porous bones may increase the weight of the skeletal remains studied (Duday et al., 2000; Depierre, 2014). Duday (in Van Andringa et al., 2013) suggests that the average total weight of a cremated archaeological individual is between 1,250 g and 1,499 g, regardless of sex. These theoretical values apply to adults and adolescents, which is consistent with our sample. Based on Duday's (in Van Andringa et al., 2013) proposed categories for the cremated remains at Porta Nocera (Pompeii), in this study, if the total weight exceeds 1,500 g the secondary cremation burial is considered to have been of an individual with a high total weight overall.

It is important to note that the overall weight of cremated remains is influenced not only by the actual weight of the skeleton, but also by various funeral-related factors such as temperature and collection type (total or partial) (Duday, 2019; Duday et al., 2000). Factors like the state of conservation and rates of fragmentation can also have an impact on the total weight analysed, so that identifying specific anatomical areas is challenging. Therefore, differential identifications based on anatomical regions and theoretical weight indexes becomes crucial. For example, diaphyseal fragments of long bones are often classified as indeterminate when they cannot be attributed to a specific bone (Duday et al., 2000). In our study, we focused on not just the total cremation weight but also prioritized the trunk weight index, which has a theoretical reference value of 17%. This specific region was chosen because it has higher identification rates than other anatomical regions (Duday et al., 2000), and due to the higher frequency of bone alterations potentially related to fluorosis based on the protocol proposed in this study.

Detecting fluoride in cremated remains: applicability of Laser-induced breakdown spectroscopy (LIBS)

As a consequence of its pronounced electronegativity, fluoride has a natural affinity for calcium hydroxyapatite ($Ca_{10}(PO_4)_6(OH)_2$)[7] (Miller and Phillips, 1953; 1956). After intake, fluorine passes through blood or the gastrointestinal tract and is then rapidly incorporated into calcified tissues, which contain up to 99% of body fluorine (Whitford, 1994; Zohoori and Duckworth, 2017). The hydroxyl ions of hydroxyapatite crystals are then replaced by fluoride, converting the hydroxyapatite into fluorapatite and consequently producing changes in the physical characteristics of the crystals (WHO, 1992; Barbier et al., 2010; Ghosh et al., 2013).

Fluoride is a halogen gas with a low atomic number, which means that its detection requires very accurate and reliable analytical methods. In previous palaeopathological studies of bone fragments from inhumations, fluoride has been detected using methods such as atomic absorption spectrometry (AAS) (Littleton, 1999), instrumental neutron activation analysis (INAA) (Petrone et al., 2011; 2013), ion-selective electrodes (ISE) (Yoshimura et al., 2006; Walser et al., 2020) or electron microprobes (EMP) (Zhou et al., 2023). All these methods allow the fluoride content to be measured, but they also require the extraction and destruction of the samples to perform the analysis. To overcome this limitation, we used laser-induced breakdown spectroscopy (LIBS), a method for elemental detection recently introduced in archaeometry. This method is sensitive enough to detect elements qualitatively, particularly halogens or light elements (Gaft et al., 2014; Pořízka et al., 2017). In addition, it can measure quantitative concentrations at around the part-per-million (ppm) level by combining LIBS with other methods (Rehse et al., 2012; Spizzichino and Fantoni, 2014). Furthermore, its potential for use with unprepared samples (Rehse et al., 2012; Álvarez et al., 2014; Alvarez-Llamas et al., 2017), its portability and its nano-destructive nature ensure a minimally invasive approach to data collection (Syvilay et al., 2019).

The LIBS method relies on a brief laser pulse (lasting nanoseconds - Ns - or less) directed at a small area of the sample (approximately 100-200 µm in diameter). This process leads to sample ablation and the formation of a dynamic laser-induced plasma. An optical emission spectrometer is then used to measure the radiation emitted from the excited plasma species (Alvarez-Llamas et al., 2016). The most intense emission lines of fluoride lie at wavelengths shorter than 100 nm, which standard LIBS spectrometer set-ups using atmospheric air cannot detect (Alvarez-Llamas et al., 2016). Therefore, for this study, we used CaF I molecular emission bands at 535 nm (Álvarez et al., 2014).

The portable instrument used is an EasyLIBS from IVEA Solution, equipped with a Nd:YAG laser at 1064 nm with a frequency of 1 Hz. The pulses delivered are 5 ns and 30 mJ. The plasma is collected via optical fibres connected to three separate compact Czerny-Turner spectrometers

7 Hydroxyapatite is the main inorganic content of bone. Bone is a biocomposite of inorganic component (50%-70%), organic component (20%-40%), water (5%-10%) and lipids (approximately 3%) (Rho et al., 1998; Boskey, 2007; Talal et al., 2020).

(Ocean Optics), which cover a spectral range between 200 and 1013 nm, with a spectral resolution of 0.2 nm. The analysis distance was set at 10 cm.

LIBS models for analysis of non-prepared samples are based on solid homogeneous specimens (Jantzi et al., 2016). Femurs have wider and more homogeneous cortical sections, a significantly higher fluoride content compared to other bones (Turkekul et al., 2020) and a slow cortical turnover rate (5%/year) (Parfitt, 2002; Lerebours et al., 2020). Therefore, one femur fragment from each individual in the Cumae sample and the control sample were analysed using the following protocol: 6 measurement points per sample, with 50 laser shots per point. The spectra processing to obtain an average spectrum for each sample was then carried out with LIBStick software, developed by one of us (YL) (https://github.com/crp2a/LIBStick). The initial ten spectra were excluded to remove pollution and alterations from the surface. Subsequently, the spectral data were processed based on the simple measurement of CaF I molecular emission within the 525-562 nm range and standardised, resulting in intensities expressed in arbitrary units (a.u.). These baseline-subtracted signals are therefore semi-quantitative data that allow comparisons of intensities within the sample analysed.

Multivariate analysis

A comparative multivariate analysis was conducted using R v.4.1.3, incorporating the following categories as variables: "total cremation weight", "trunk weight index", "LIBS measurements" and "suspicion". The aim of this analysis was to explore the relationships between the study sample and the various criteria used for diagnosing fluorosis. The multivariate techniques used, including cluster analysis and principal component analysis (PCA), were applied to identify systematic relationships among the variables, as well as to examine the nature of these relationships.

Results

Palaeopathological observations and suspicion of fluorosis

Applying the macroscopic observation protocol to the Cumae sample enabled us to identify various pathological changes, some of which are illustrated in figure 4. The specific details of lesions observed for each individual are given in table 3. The twelve anatomical regions observed were unequally affected by pathological changes, with the prevalence of lesions as follows (from the lowest value to the highest): 13% for the wrist (2/15), 22% for both the cranial vault (9/41) and the glenohumeral joint (7/32), 40% for the ribs (17/42), 45% for both the patella (9/20) and the tibia (5/11), 46% for the pelvic girdle (17/37), 48% for the elbow joint (10/21), 53% for the sternum (9/17), 67% for the femur (26/39), 70% for the vertebrae (30/43) and 82% for the calcaneus (14/17).

Nine individuals were excluded from category attribution because observations could only be made in less than five anatomical areas. These account for 21.7% of the total sample. Among the remaining individuals (n=36), 39% are males (n=12) or probably males (n=2), and 58% are females (n=19) or probably females (n=2). In 51% of the Cumae sample, observations could be made in eight or more anatomical zones, *i.e.* at least two thirds of the areas considered in our protocol.

Among the samples to which a category of fluorosis suspicion could be attributed, the results are as follows: 13 individuals (36%) have "no suspicion", 14 (39%) were placed in the "moderate suspicion" group and 9 (25%) in the "strong suspicion" group (figure 5A). All sex groups are represented among the three categories of fluorosis suspicion in this study. However, as shown in figure 5, the representation of female individuals in the "strong suspicion" category is notably lower (n=2).

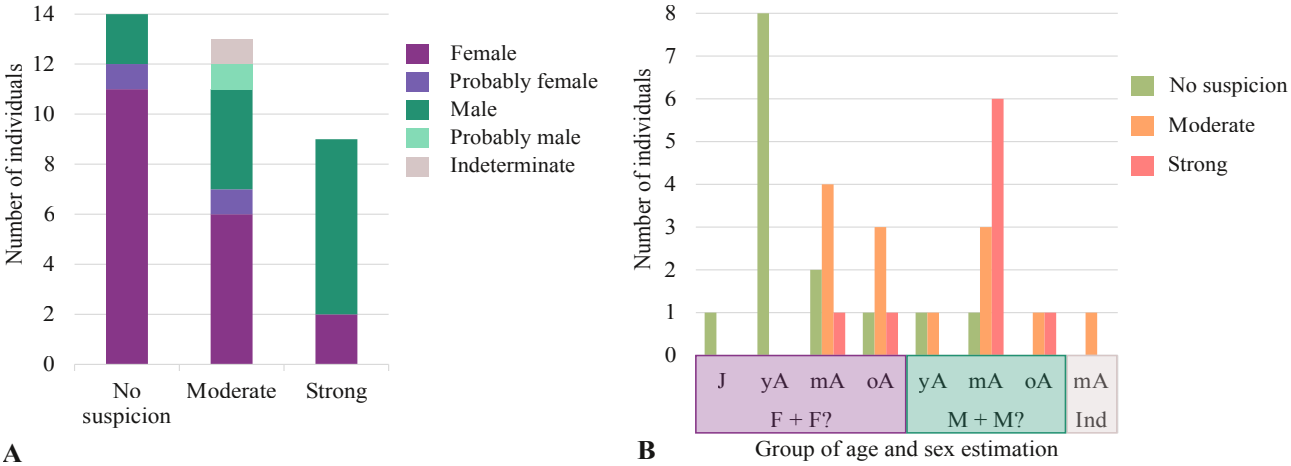

Figure 5. Fluorosis suspicion in the Cumae sample. A) Fluorosis suspicion and sex distribution; B) Sex and age distribution correlated with fluorosis suspicion / *Suspicion de fluorose dans l'échantillon de Cumes. A) Distribution de suspicion de fluorose par sexe ; B) Répartition par classe d'âge et sexe corrélé à la suspicion de fluorose*

Sample ID	Cranial vault	Glenohumeral joint	Elbow joint	Wrist	Ribs	Sternum	Vertebrae	Pelvic girdle	Femur	Patella	Tibia	Calcaneus	n Obs	n P	% P	Fluorosis suspicion
CU2001	A	NO	NO	A	P	P	P	P	A	NO	A	P	9	5	56	2
CU29008	A	A	NO	NO	A	A	A	A	A	NO	NO	NO	7	0	0	1
CU29014	A	NO	A	NO	P	A	P	A	A	A	NO	NO	8	2	25	1
CU29050	A	P	P	P	P	P	P	P	P	P	P	P	12	11	92	3
CU29060	A	NO	NO	NO	A	NO	A	A	NO	A	A	P	7	1	14	1
CU34174	A	A	NO	NO	A	NO	P	A	P	NO	NO	NO	6	2	33	2
CU34220	A	A	P	NO	P	P	P	P	P	P	NO	P	10	8	80	3
CU34241	A	A	A	A	A	NO	A	A	P	A	NO	P	10	2	20	1
CU34242	A	NO	NO	NO	A	NO	P	P	A	NO	NO	NO	5	2	40	2
CU34247	A	A	NO	NO	A	NO	P	NO	A	NO	P	NO	6	2	33	2
CU34276	P	P	P	A	P	NO	P	P	P	NO	NO	P	9	8	89	3
CU34279	A	P	A	A	P	P	P	P	P	P	A	P	12	8	67	2
CU34283	P	A	P	NO	A	A	P	P	P	P	A	P	11	7	64	2
CU34243	NO	NO	NO	NO	P	P	P	P	P	NO	NO	NO	5	5	100	3
CU34253	P	NO	NO	NO	P	NO	P	NO	P	NO	NO	NO	4	4		NA
CU35335	A	A	NO	NO	A	NO	A	A	P	NO	NO	NO	6	1	17	1
CU35370	A	A	P	NO	P	NO	P	A	P	A	A	P	10	5	50	2
CU35381	A	A	A	A	A	NO	A	A	A	A	A	NO	10	0	0	1
CU35383_35415	P	NO	NO	NO	A	NO	P	NO	NO	A	NO	NO	4	2	50	NA
CU35384	A	A	NO	A	A	NO	P	A	P	NO	NO	NO	7	2	29	1
CU35389	A	A	A	NO	A	NO	NO	NO	NO	NO	NO	NO	4	0		NA
CU35398	P	NO	NO	NO	NO	NO	A	A	A	NO	NO	NO	4	1		NA
CU35410	A	A	A	NO	P	NO	A	A	A	NO	NO	NO	7	1	14	1
CU35414	A	A	A	A	A	NO	P	NO	P	NO	NO	NO	7	2	29	1
CU35417	P	P	P	P	P	P	P	P	P	P	NO	P	11	11	100	3
CU35429	A	NO	NO	NO	A	NO	A	NO	NO	NO	NO	NO	3	0		NA
CU35482	P	P	P	A	P	P	P	P	P	P	NO	P	11	10	91	3
CU35456	A	A	NO	A	A	A	P	P	P	A	NO	NO	9	3	33	2
CU35461	A	A	P	NO	A	NO	P	P	P	A	NO	A	9	4	44	2
CU35478	A	A	A	NO	A	A	P	A	A	NO	NO	NO	8	1	13	1
CU35490	A	A	NO	NO	P	NO	P	P	P	NO	NO	A	7	4	57	2
CU37043	A	A	A	A	A	A	A	A	A	A	NO	NO	10	0	0	1
CU37044	P	P	A	A	P	P	P	P	P	A	P	P	12	9	75	3
CU37045	P	A	NO	NO	P	A	P	P	P	NO	P	NO	8	6	75	3
CU39392	A	NO	NO	NO	A	NO	P	A	P	NO	NO	NO	5	2	40	2
CU39186	NO	NO	NO	NO	A	NO	A	NO	NO	NO	NO	NO	2	0		NA
CU39305	A	NO	P	A	A	NO	P	A	P	P	NO	P	9	5	56	2
CU39306	A	P	P	NO	P	P	P	P	P	P	NO	P	10	9	90	3
CU39353	NO	A	NO	NO	NO	NO	NO	A	P	NO	NO	NO	3	1		NA
CU39381	NO	A	NO	NO	NO	NO	P	A	A	NO	NO	NO	4	1		NA
CU39389	A	A	NO	NO	A	NO	A	A	NO	NO	NO	NO	5	0	0	1
CU39390	A	NO	NO	NO	A	NO	P	NO	P	NO	NO	NO	4	2		NA
CU39391	A	A	A	NO	A	NO	A	P	A	P	NO	NO	8	2	25	1
CU39396	A	A	NO	NO	P	A	P	A	P	NO	P	NO	8	4	50	2
CU39397	A	A	NO	A	A	NO	A	A	A	A	NO	A	9	0	0	1

Table 3. Palaeopathological observations. Legend: Pathological alterations in the twelve anatomical zones observed: A = absent, P = present, NO = non-observable, n Obs = total number observable, n P = total number present, % P = relative frequencies of present within the observable total. Fluorosis suspicion: 1 = no suspicion, 2 = moderate, 3 = strong, NA = non-attributable / *Observations paléopathologiques. Légende : Altérations pathologiques dans les douze zones anatomiques observées : A = absente, P = présente, NO = non observable, n Obs = nombre total observable, n P = nombre total présent, % P = fréquences relatives des présentes dans le total observable. Suspicion de fluorose : 1 = sans suspicion, 2 = modérée, 3 = forte, NA = non attribuable*

Figure 5B shows the correlation between age group and categories of fluorosis suspicion. These results indicate that no juveniles and only one young adult present bone signs suggestive of fluorosis. In contrast, bone lesions suggesting a moderate or strong suspicion of fluorosis are common in middle-aged and elderly individuals. A detailed view of the "strong suspicion" category indicates that it is more frequent among male individuals over 30 years old. Additionally, the ratio between strong and moderate suspicion is higher in the middle-aged adult group (7:8) than in the elderly adult group (2:4).

When we analyse the distribution and relative frequencies of pathological bone changes in the "moderate suspicion" and "strong suspicion" groups in our sample (n=22), our observations show similar results to those from previously published studies (Littleton, 1999; Petrone et al., 2013; Nelson et al., 2019). The thoracic anatomical zones are more affected overall than the cranial vault and upper limbs. After changes observed in the vertebrae, the most characteristic alterations were seen in the lower limb anatomical zones, particularly on the femur and pelvic girdle. The higher frequency for the calcaneus is also comparable to the results of Littleton (1999); however, our higher value can also be attributed to the large and well-preserved fragments, where calcaneal tuberosities can be very clearly distinguished (table 4).

Anatomical zone	n P/ n Obs	% (relative Obs)
Cranial vault	6/21	29%
Glenohumeral joint	7/17	41%
Elbow joint	10/12	83%
Wrist	2/9	22%
Ribs	14/22	64%
Sternum	9/13	69%
Vertebrae	22/22	100%
Pelvic girdle	16/21	76%
Femur	19/22	86%
Patella	8/12	67%
Tibia	5/9	56%
Calcaneus	12/14	86%

Table 4. Relative frequency of pathological bone alterations in the "moderate and strong suspicion" groups. Legend: *n* P = number of individuals with pathological alterations present, *n* Obs = number of individuals where the anatomical zone can be observed, % (relative Obs) = relative frequency of the number of individuals with pathological alterations / *Fréquence relative des lésions ostéologiques pour les groupes de suspicion modérée et forte. Légende : n P = nombre d'individus présentant des lésions ostéologiques, n Obs = nombre d'individus où la zone anatomique peut être observée, % (Obs relative) = fréquence relative du nombre d'individus présentant des lésions ostéologiques*

Correlation of cremation data and suspicion of fluorosis

In the graphs shown in figure 6, each category of fluorosis suspicion is represented within the correlation of total cremation weight (x-axis) and trunk weight index (y-axis). In the "no suspicion" (figure 6A) and "moderate suspicion" (figure 6B) groups, it is notable that some individuals exceed the theoretical value for the trunk weight index and/or average value for the total weight. Among the individuals in the "no suspicion" group, the highest total weight recorded is 1,847.2 g, belonging to an older adolescent female (CU34241). In the "moderate suspicion" group, there is slightly greater dispersion, with four individuals showing a higher trunk index and total weight overall. The highest weights recorded are around 2,000 g, corresponding respectively to a young adult male (CU35370) and two middle-aged adult females (CU39396 and CU34283). The data dispersion in the "strong suspicion" group (figure 6C) is clearly different, with seven male individuals above the theoretical values for both trunk index and total weight. The two individuals with a lower total weight are females (CU37045 and CU35482), but they both have a significantly higher value for trunk weight index. CU37045 is a noteworthy case, as this individual is an older adult female whose lower total weight could suggest a natural demineralisation process specific to the menopause (see Duday in Van Andringa et al., 2013).

Fluoride detection by LIBS

The control sample analyses were crucial to identify average fluoride values for individuals from non-volcanic contexts with no suspicion of fluorosis, whether they were cremated or not. Results from LIBS analyses have confirmed the potential of this method for studies of cremated human remains, including fluoride detection. The results obtained for the Cumae sample reinforce our palaeopathogical protocol and our proposed division into categories of suspicion.

Figure 7 illustrates the correlation of the LIBS results with the three categories of suspicion outlined in this study. The results indicate that our control sample has lower LIBS values compared to the Cumae sample, whose overall values are significantly higher. The control sample values range from 0.0160 to 0.0258 a.u. ($\bar{x}$=0.0220, σ=0.0041); the Cumae sample values are higher and range from 0.0372 to 0.1616 a.u. ($\bar{x}$=0.0878, σ=0.0366) (table 5). The elevated levels of fluoride in the Cumae population may be attributed to environmental contributions associated with the underlying volcanic system and therefore with nutrient intake, most probably through the consumption groundwater, which is a primary source of fluoride for humans (Barbier et al., 2010; Baxter and Horwell, 2015; Yeşilnacar et al., 2016).

A close examination of the LIBS values for each suspicion category (no suspicion, moderate, strong) shows that our palaeopathological protocol classifying subjects into

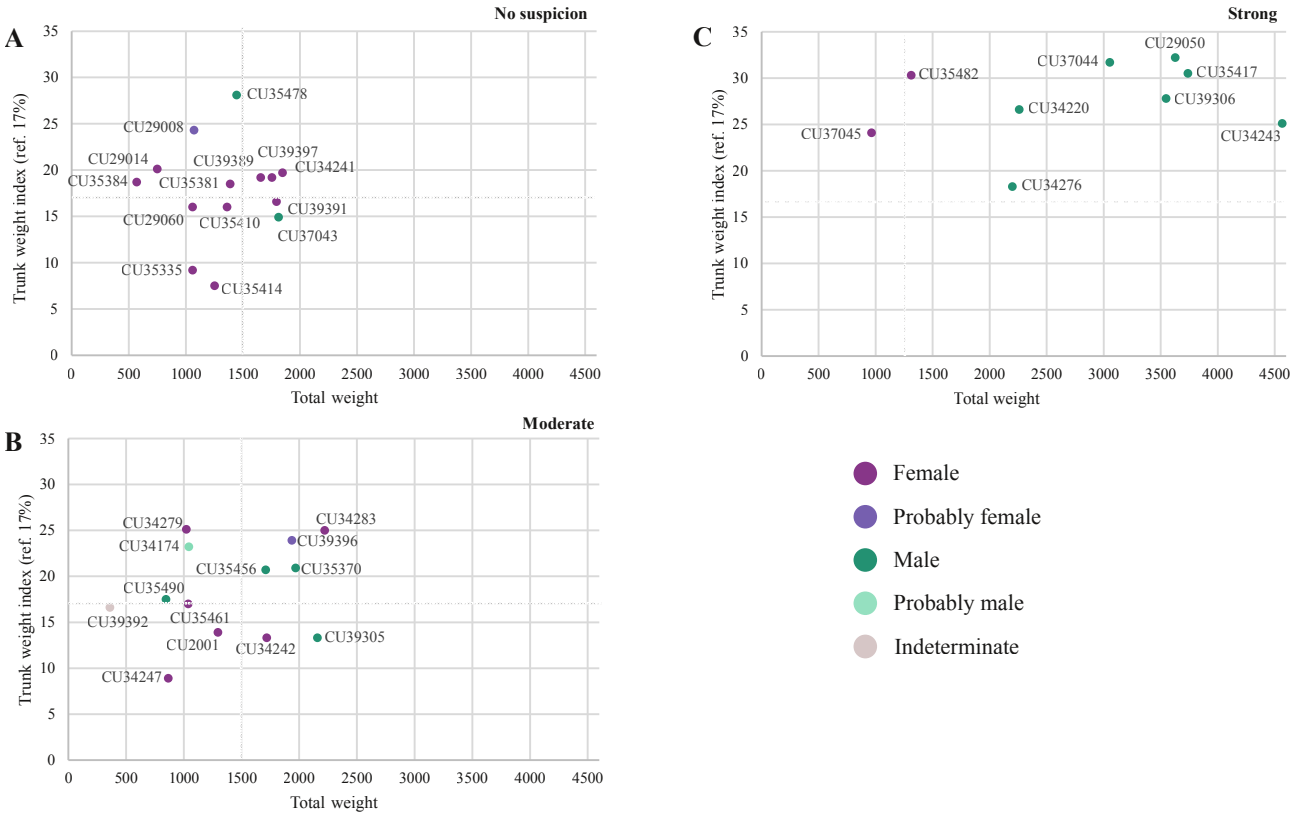

Figure 6. Total trunk weight index and total burnt bones weight correlated with the different categories of fluorosis suspicion. A) Correlation for the "no suspicion" group; B) Correlation for the individuals with "moderate suspicion"; C) Correlation for the "strong suspicion" group. The dotted line on the x-axis shows the average normal total weight (1,500 g) and the dotted line on the y-axis shows the theoretical trunk weight index (17%) / *Indice pondéral du tronc et masse totale des os humains brûlés corrélés aux différentes catégories de suspicion de fluorose. A) Corrélation pour le groupe sans suspicion ; B) Corrélation pour les individus avec suspicion modérée ; C) Corrélation pour le groupe de suspicion forte. La ligne pointillée sur l'axe x montre la masse totale moyenne (1 500 g) et la ligne pointillée sur l'axe y montre l'indice pondéral théorique du tronc (17 %)*

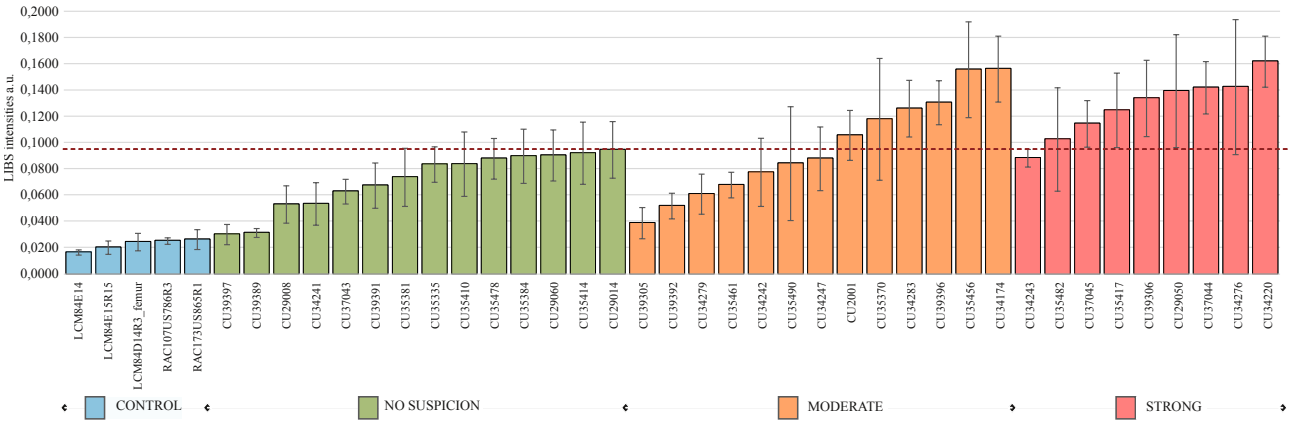

Figure 7. Cross-analysis of data from palaeopathological observations by category of suspicion and LIBS measurements. The dotted line shows the proposed threshold for a strong suspicion of fluorosis / *Analyse croisée des données d'observations paléopathologiques par catégorie de suspicion et mesures LIBS. La ligne pointillée montre le seuil proposé pour une forte suspicion de fluorose*

groups indeed correlates with fluoride detection (table 5) and is therefore relevant when attempting to diagnose fluoride poisoning. The "no suspicion" group has the lowest values with an average of 0.0706 a.u. (σ=0.0220), followed by the moderate and strong suspicion groups, with averages of 0.0966 a.u. (σ=0.0384) and 0.1274 a.u. (σ=0.0228) respectively.

Since our sample consists only of older adolescents and adults, the results can be analysed by sex (see details in table 5). Hereafter, we include both "female" and "probably female" in the female group, and likewise for male individuals. The mean values for females are 0.0698 a.u. (σ=0.0233) for "no suspicion", 0.0934 a.u. (σ=0.0277) and 0.1082 a.u. (σ=0.0084) for "moderate" and "strong

Sample ID	Fluorosis suspicion category	Sex estimation	LIBS measurements	
			CaF simple measurement [529-534,5] normalized (a.u.)	σ
LCM84E14	0	?	0.0160	0.0020
LCM84E15R5	0	?	0.0197	0.0051
LCM84D14R3_femur	0	?	0.0239	0.0067
RAC107US786R3	0	?	0.0247	0.0025
RAC173US865R1	0	?	0.0258	0.0076
CU35398	NA	F?	0.0372	0.0069
CU39390	NA	F?	0.0446	0.0110
CU39186	NA	Ind	0.0488	0.0200
CU34253	NA	M?	0.0495	0.0110
CU35429	NA	Ind	0.0536	0.0169
CU35389	NA	Ind	0.0554	0.0164
CU35383_35415	NA	F	0.0623	0.0249
CU39353	NA	F	0.0853	0.0240
CU39381	NA	M	0.1236	0.0117
CU39397	1	F	0.0297	0.0077
CU39389	1	F	0.0308	0.0034
CU29008	1	F?	0.0526	0.0142
CU34241	1	F	0.0530	0.0162
CU37043	1	M	0.0624	0.0094
CU39391	1	F	0.0670	0.0173
CU35381	1	F	0.0733	0.0222
CU35335	1	F	0.0831	0.0135
CU35410	1	F	0.0833	0.0246
CU35478	1	M	0.0875	0.0155
CU35384	1	F	0.0894	0.0207
CU29060	1	F	0.0900	0.0195
CU35414	1	F	0.0917	0.0237
CU29014	1	F	0.0942	0.0216
CU39305	2	M	0.0383	0.0119
CU39392	2	Ind	0.0514	0.0098
CU34279	2	F	0.0605	0.0153
CU35461	2	F	0.0674	0.0098
CU34242	2	F	0.0771	0.0260
CU35490	2	M	0.0838	0.0434
CU34247	2	F	0.0875	0.0243
CU2001	2	F	0.1053	0.0190
CU35370	2	M	0.1176	0.0465
CU34283	2	F	0.1257	0.0216
CU39396	2	F?	0.1302	0.0168
CU35456	2	M	0.1554	0.0365
CU34174	2	M?	0.1559	0.0252
CU34243	3	M	0.0879	0.0067
CU35482	3	F	0.1022	0.0395
CU37045	3	F	0.1141	0.0178
CU35417	3	M	0.1244	0.0284
CU39306	3	M	0.1335	0.0291
CU29050	3	M	0.1391	0.0431
CU37044	3	M	0.1416	0.0200
CU34276	3	M	0.1422	0.0515
CU34220	3	M	0.1616	0.0195

Table 5. LIBS measurement results. Legend: Suspicion of fluorosis: 0 = control sample, 1 = no suspicion, 2 = moderate, 3 = strong, NA = non-attributable. Sex: Ind = indeterminate, F = female, F? = Probably female, M = male, M? = probably male, - = not identified / *Résultats des mesures LIBS. Légende : Suspicion de fluorose : 0 = échantillon contrôle, 1 = sans suspicion, 2 = modérée, 3 = forte, NA = non attribuable. Diagnose sexuelle : Ind= indéterminé, F = féminin, F? = féminin probable, M = masculin, M ? = masculin probable, - = non identifié*

suspicion", whereas for males they are respectively as follows: 0.0750 a.u. (σ=0.0177), 0.1102 a.u. (σ=0.0501), 0.1329 a.u. (σ=0.0228). From the data analysis, it is evident that the average values for male individuals consistently exceed those for female individuals across all categories. However, this difference between the sexes appears to widen with increasing levels of suspicion. Specifically, the difference between male and female averages is three times greater in the "moderate suspicion" group (0.0168) than in the "no suspicion" group (0.0051), and roughly one-and-a-half times greater in the "strong suspicion" group (0.0248) than in the "moderate suspicion" group.

A Mann-Whitney non-parametric test (*U* test) was performed to evaluate the differences between sample groups. There is a highly significant difference between the Cumae sample and the control sample (p=0.00038). When comparing two contiguous groups (no suspicion vs. moderate; moderate vs. strong) there is no significant difference (p=0.120 and p=0.153, respectively). However, there is a significant difference when comparing the "no suspicion" group with the "moderate" and "strong suspicion" groups together, and also when comparing the "strong suspicion" group with the rest of the Cumae sample (p=0.00705 and p=0.00729, respectively). Furthermore, there is also a significant difference in LIBS values between males and females (p=0.02996).

Among the three categories of suspicion, there is higher variability in the "moderate" category. The LIBS values for this group overlap with both the "no suspicion" and "strong suspicion" categories (figure 7). These results do not offer a definitive differentiation of this category based solely on LIBS, but they do emphasise the importance of incorporating anthropological observations with this method. They also raise the question of the pertinence of this category in terms of its osteological reality, suggesting that it may need further evaluation with additional skeletal and clinical evidence.

Upon thorough analysis of the findings, it becomes evident that the LIBS values allow for a clear separation between the "no suspicion" and the "strong suspicion" groups (figure 7). We propose that the cut-off point for identifying definite cases of fluorosis can be established by using the maximum measurement possible in the sample with the lowest intensity value in the "strong suspicion" category (CU34243: $\bar{x}$=0.0879, σ=0.0067, max.=0.0946) and rounding it to three decimal points (i.e. 0.095 a.u.; figure 7). This threshold could serve as a baseline for future studies of populations from the same geological context.

Multivariate analysis

Figure 8 shows the results of the multivariate analysis. The hierarchical tree (figure 8A) reveals three main groups. The Principal Component Analysis (PCA) scatter-plot (figure 8B), with the first two components, explains 80.53% of the variance (63.86% and 16.67%). The trunk weight index is strongly correlated with the suspicion variable (r=0.562, $p < 0.01$).

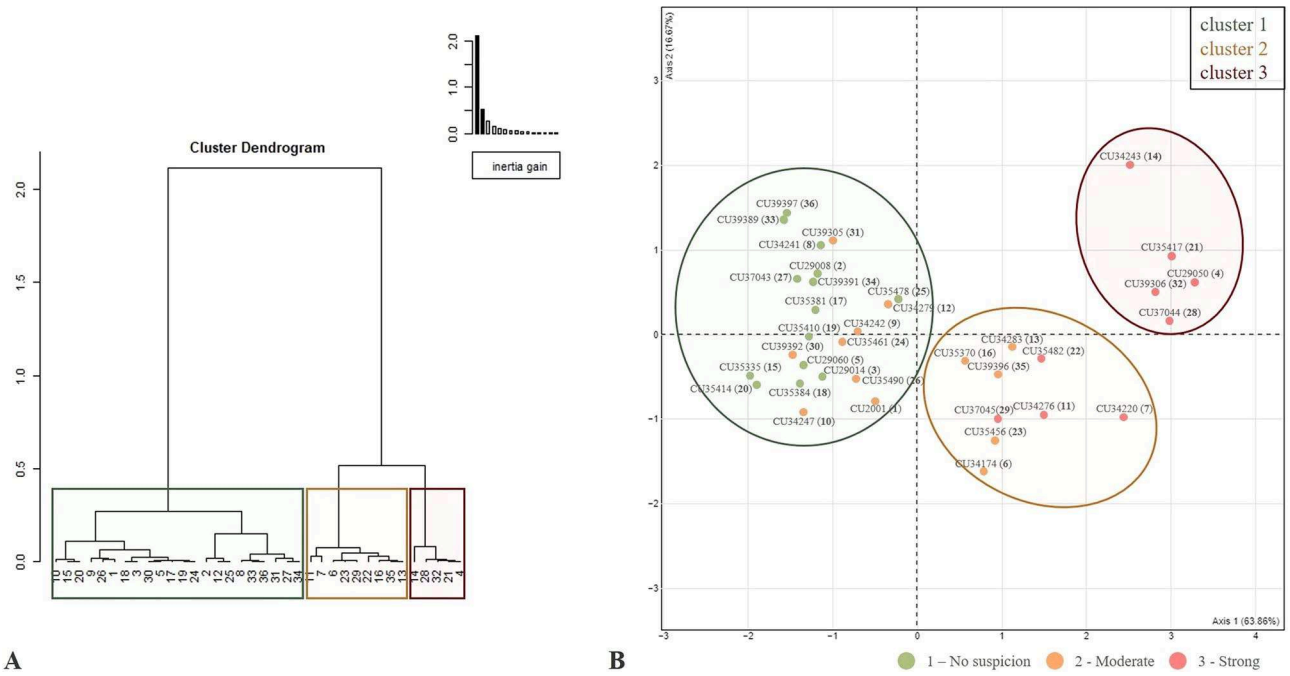

Figure 8. A) Hierarchical clustering tree illustrating the classification of individuals into three distinct clusters; B) PCA scatter-plot depicting the distribution of individuals within each cluster, with categories of suspicion indicated for each individual. In brackets, the individual number corresponding to those indicated in the hierarchical clustering tree / *A) Arbre de classification hiérarchique illustrant la répartition des individus en trois clusters distincts ; B) Diagramme de dispersion en ACP montrant la répartition des individus au sein de chaque cluster, avec les catégories de suspicion indiquées pour chaque individu. Entre parenthèses, le numéro de l'individu correspondant à ceux indiqués dans l'arbre de classification hiérarchique*

Cluster 1 comprises all "no suspicion" individuals and eight "moderate suspicion" individuals. This cluster is characterised by low values for the "LIBS measurements", "trunk weight index", and "total cremation weight" variables, in order from the lowest to the highest. Cluster 2 is distinguished by high values for the "LIBS measurements" and "trunk weight index" variables, with individuals in this cluster exhibiting moderate (n=5) and strong (n=4) suspicion. Cluster 3 is made up of "strong suspicion" individuals and is marked by high values for the "total cremation weight", "trunk weight index" and "LIBS measurements" variables, in order from the highest to the lowest.

Discussion

Palaeopathology protocol and bone modifications

This analysis demonstrates that the bone changes noted in the Cumae sample, the correlation with cremation data (total weight and trunk weight index) and the LIBS measurements are probably indicative of skeletal fluorosis, particularly for those categorised under "strong suspicion". It should be noted that some of the bone lesions recorded can also be associated with other pathological conditions (see table 2). Most of these disorders, such as myositis ossificans progressiva, Paget's disease, hypoparathyroidism, osteopetrosis, treponematoses and hematogenous osteomyelitis can be readily ruled out. These conditions are rare and/or result in bone changes that are not present in the Cumae individuals (see Supplementary Information for a detailed differential diagnosis). Diffuse idiopathic skeletal hyperostosis and ankylosing spondylitis can cause a mosaic of bone changes resembling those in skeletal fluorosis, so they cannot be definitely excluded. However, these latter conditions are unlikely to be found in such a large proportion of individuals and would most certainly not result in elevated fluoride levels. Based on this differential diagnosis, the most probable cause of the bone modifications recorded throughout the Cumae sample is skeletal fluorosis. However, since the changes caused by skeletal fluorosis are gradual, we cannot rule out the possibility that some of the bone modifications observed may have arisen from osteoarthritis or been exacerbated by normal mechanical demands and age-related degenerative processes.

Although the protocol proposed was applied to cremated remains, our results for bone lesions are consistent with those from other archaeological contexts where the remains do not show signs of burning (Callaghan, 1986; Littleton, 1999; Weinstein, 2005; Yoshimura et al., 2006; Petrone et al., 2013; Nelson, 2015; Nelson et al., 2016; 2019; Walser et al., 2020; Zhou et al., 2023), as well as with those from clinical studies (*e.g.* Jolly et al., 1968; Brickley and Ives, 2008a; Datta and Datta, 2013; Sellami et al., 2020).

It seems evident that one of the anatomical areas most affected by bone modifications is the trunk. As seen on the Cumae sample, the relative frequencies of bone alterations observed are 100%, 69% and 64% for the vertebrae, sternum and ribs, respectively. These results, besides being similar to those from previous palaeopathological studies (Littleton, 1999; Petrone et al., 2013; Nelson et al., 2019), are also consistent with radiological data for the diagnosis of skeletal fluorosis in living patients (Sellami et al., 2020). We can also infer that the higher prevalence in this specific anatomical region is consistent with bone biology, as this area contains multiple zones with connective tissue and is therefore prone to ossification (de Vlam et al., 2006).

The fact that the second most affected area is the lower limb, more specifically the femur (86%), is likewise consistent with typical skeletal fluorosis bone alterations (Littleton, 1999; Nelson et al., 2019). Furthermore, in addition to the observations proposed in our protocol, we were able to observe sections of femoral diaphysis and note that the cortical bone was abnormally thick (figure 4I). Abnormal bone formation is related to osteosclerotic changes (de Vlam et al., 2006), and is therefore responsible for the abnormal weight or "heaviness" characteristics that we observed among the individuals of the Cumae sample.

Although our sample is small, our results show that bone alterations are higher amongst males than females. This observed sex difference in fluorosis may be linked to various factors in the variables studied for diagnosing this condition. Some lesions attributed to fluorosis could be due to age-related degenerative changes or traits associated with robustness, especially when the diagnosis relies solely on osteological features.

Additionally, data on total cremation weight and trunk weight index also suggest a higher prevalence in males. However, these findings may be biased when considered separately. The robustness often attributed to males could lead to an overestimation of the prevalence rate in males, which is a significant limitation in sex estimations of cremated remains (Duday et al., 2000). From a statistical perspective, using fixed thresholds based on theoretical references might underestimate the number of females.

It is important to note that LIBS results are not influenced by the aforementioned variables and exhibit the same trend, as shown by the multivariate analysis. Consequently, the demographic data appears to be reliable, as it is supported by evidence unaffected by these biases. However, the underrepresentation of older adult females in the sample is a significant limitation that could influence the results.

While many clinical and palaeopathological studies support a higher prevalence of skeletal fluorosis in males, the underlying causes of this observed difference require further investigation (*e.g.* sexually dimorphic biology or behaviour, Walser et al., 2020). For instance, clinical research by Mohammadi and collaborators (2017) on an Iranian population found a higher prevalence in females. Moreover, hormonal changes during menopause in adult females might also be a factor to consider. Duday (in Van Andringa et al., 2013) has already discussed that this female specificity can affect the total weight of cremated remains, but there is also the possibility that natural demineralisation can

mask some bone modifications and an overall diagnosis of fluorosis, whether in cremated or non-cremated remains or even in clinical samples. Although the limited number of females in our sample reduces support for this hypothesis at present, further research is needed to fully explore this potential explanation. Before doing so, additional research on the mineral density (Yildiz and Oral, 2003) and micro-architecture of cremated remains should be carried out (by microtomographic analyses for example).

When considering the data by age group, it seems that the rarity of strong suspicion of fluorosis among the youngest individuals in the sample (juvenile and young adults) may be linked to the duration of exposure and the time necessary to develop bone signs. A higher occurrence of strong suspicion of fluorosis was observed in the individuals over 30 years old (especially in the middle-aged adult group); these results also correspond to clinical studies that report a higher occurrence of skeletal fluorosis from around 30 to 40 years of age and beyond (Datta and Datta, 2013; Sellami et al., 2020). Similarly, our findings align with Littleton's results (1999), which indicate that few bone lesions are observed before the age of 30. However, it is important to stress that there is a potential bias: because skeletal fluorosis is an age-related condition, it is difficult to isolate bone lesions caused by aging from those caused by fluorosis, particularly with fragmented remains. Consequently, the risk of false positives increases with age, as older individuals are more likely to develop osteophytes, enthesophytes and similar conditions. This difficulty underscores the importance of combining macroscopic observations with archaeometric analysis. Furthermore, while robusticity and age-related changes do not account for all the features observed (*e.g.* thickened diploe and certain forms of bone densification), they do play a significant role in many of the lesions or features detected, including porosity, bone densification and the development of enthesophytes and osteophytes. These age-related changes are most commonly seen in the spine and lower limb areas, which are particularly susceptible to fluorosis. However, it is important to recognise that some features observed in individuals are not attributable to aging.

The main challenges for this research were to study a pathological condition with no pathognomonic lesions, and dealing with the nature of our sample. Cremated remains, as stated in previous sections, can limit observations due to their fragmentary state and incomplete representations of anatomical areas. However, by incorporating the average total weight and weight indexes for the different anatomical areas into the proposed protocol, more comprehensive interpretations can be achieved. The findings in this study, including the multivariate analysis, reveal a significant correlation between the trunk weight index and the cases of strong suspicion of fluorosis. This anatomical area not only has higher rates of identification among cremated remains (Duday et al., 2000), but also a higher relative frequency of the pathological changes identified in this study (see table 4). The correlation results demonstrate a clear association between these two sets of cremation data, when weights exceed both the overall average normal total weight (1,500 g) and the trunk weight index (17%), supporting a strong suspicion of fluorosis. In contrast, there is greater variation in the results for the "no suspicion" and "moderate suspicion" categories, which makes the correlations established less conclusive. Further research is necessary to determine whether higher weight values in these categories should be attributed to factors other than pathology.

LIBS contribution and potential for fluoride detection

Our findings demonstrate that fluoride can be effectively detected by laser-induced breakdown spectroscopy (LIBS). The use of LIBS in our study is pivotal, as it produces a more accurate determination of the origins of the skeletal lesions observed. Without this elemental analysis, drawing conclusions about their aetiology would have been difficult. Additionally, our application of this innovative methodology represents a significant contribution to the field.

As proposed by previous researchers, emissions from CaF bands (around 535 nm) offer a viable alternative for accurately detecting and assessing fluoride levels (Álvarez et al., 2014; Alvarez-Llamas et al., 2016; Pořízka et al., 2017; Foucaud et al., 2019), and this method can also be applied to cremated human remains. Our current research shows that LIBS has promising potential as a method for elemental analysis. Its portability enables analyses to be conducted both in the field and in the laboratory. Our findings also show its potential for application to archaeometric studies relating to questions in biological anthropology, complementing its existing uses in areas such as art history (Spizzichino and Fantoni, 2014) and biomedicine (Samek et al., 2001). However, it must be noted that LIBS is a relatively new technique which is still undergoing development and improvement, specifically for quantitative analysis.

The control sample in this study was set up to establish a standard set of data for individuals who show no signs of fluorosis and come from non-volcanic areas with different burial practices (inhumation and burial after cremation). Apart from providing important data on the threshold for individuals not exposed to high levels of fluoride, the control group prompts an inquiry into the interaction between fluoride and fire, particularly in the context of cremation as a funerary practice. However, due to the limitations of our sample size, we cannot further explore how exposure to fire might influence fluoride fixation or loss. Nevertheless, it is apparent that in comparison to the control sample, all the Cumae individuals exhibit higher levels of fluoride, probably influenced by their environment.

Even though our results are semi-quantitative, they still allow us to identify different groups in the Cumae sample. The correlation with anthropological observations has enabled us to validate the potential of our macro-observation

protocol and the proposed categories, and to establish a threshold for identifying strong suspicions of fluorosis. Further research on larger skeletal samples from the same geological context presented in this study, as well as from other volcanic areas, would allow confirmation or adjustment of the proposed threshold, which in turn would improve the identification of suspected fluorosis using LIBS measurements.

Unfortunately, direct comparisons between our findings on fluoride detection and those of other researchers (Littleton, 1999; Petrone et al., 2013; Walser et al., 2020; Zhou et al., 2023) are not feasible due to the substantial differences in the methods used. However, we concur with their recognition of higher values for populations in volcanic environments. The higher values for the Cumae sample, as opposed to our control sample, are probably associated with fluoride poisoning.

As stated earlier, LIBS is a qualitative method with which quantitative data could be acquired by using reference samples or coupling with another quantitative method to allow the construction of calibration curves (Samek et al., 2001; Rehse et al., 2012; Spizzichino and Fantoni, 2014). Further research using a quantitative method (*e.g.* PIXE-PIGE) would allow us to explore the possibility of developing a calibration curve for detecting and quantifying fluoride in human remains. Conducting further research with a larger sample size and integrating LIBS with other quantitative methods will facilitate future investigations, allowing the Cumae values to be compared with those from other archaeological populations in the same geological context (Campanian volcanic arc), as well as in volcanic areas elsewhere in the world.

Aetiological factors for skeletal fluorosis: potential input from historical ecotoxicology

The environmental health impacts of historical water consumption are still underexplored. While bioarchaeological studies have investigated cases of poisoning due to fluoride (*e.g.* Littleton, 1999; Yoshimura et al., 2006; Petrone et al., 2011; 2013; 2019; Nelson, 2015; Nelson et al., 2016; 2019; Walser et al., 2020), arsenic (*e.g.* Özdemir et al., 2010; Fresnais et al., 2015; Galaz-Mandakovic and Rivera, 2022) and heavy metals (*e.g.* Emslie et al., 2015; Moore, 2019; Moore et al., 2021; Proctor, 2021), research into these issues is still limited. Concretion analyses have sometimes been used to investigate environmental pollution (*e.g.* Carlut et al., 2009; Delile, 2014; Benjelloun et al., 2019). However, more interdisciplinary research is essential to fully assess historical natural risks, particularly those related to water. Addressing this gap in knowledge would provide a critical entry point for the development of *historical ecotoxicology*.

Toxins, whether from natural or human sources, can be harmful even in small amounts (Sánchez-Bayo, 2011). Fluoride is a cumulative toxin that entails risks depending on the duration of exposure, amounts and sources (Ayoob and Gupta, 2006; Brickley and Ives, 2008b). Despite its benefits for dental health, the potential hazards of fluoride intake were under-appreciated until recent studies highlighted its adverse effects even at low doses (Barbier et al., 2010). The World Health Organization (WHO) has set the maximum safe fluoride concentration in drinking water at 1.5 mg/l to prevent poisoning (WHO, 1992; 2019). However, excessive fluoride intake can also occur through water used to produce crops, raise livestock or prepare foodstuffs (Chowdhury et al., 2019).

In Antiquity, groundwater consumption was common (Tölle-Kastenbein, 1993; Mays et al., 2007) and probably the primary source of fluoride intake. In Greek-era Cumae, water was collected from cisterns and wells (D'Acunto, 2020), a practice that most likely continued into the Roman period. The Serino aqueduct, constructed during the Augustan period (also known as the *Aqua Augusta*, ca. 38 BC-11 AD), supplied water to Pompeii and Herculaneum (Caputo, 2004; Dessales, 2008; 2013; Keenan-Jones, 2010a; 2010b; 2013; Döring, 2012; Linoli, 2012; Ferrari and Lamagna, 2013; Potenza, 2016). Although indirect evidence suggests that Cumae was connected to this aqueduct (*e.g.* inscriptions, lead pipes, decorative fountains) (Camodeca, 1997; Capaldi, 2007a; 2007b; 2008; Guardascione, 2007; Zevi et al., 2008; Brun and Gasparri, 2009; Gasparri, 2009; Gallo, 2015; Ferrari and Lamagna, 2016; Potenza, 2016; Ferrari et al., 2018), questions remain about whether the aqueduct actually reached Cumae and, if so, how it influenced fluoride intake. Further research with a larger sample is necessary to address these questions.

Fluoride exposure in the Phlegraean Fields has probably been a health risk since ancient times due to the high fluoride concentrations in the groundwater, driven by continuous volcanic activity (Rosi et al., 1983; Stellato et al., 2020; Cappelletti et al., 2022). Current levels (3.6-15 mg/l) (Ducci and Sellerino, 2012) far exceed safe drinking standards, suggesting that Roman-era water had similarly high fluoride levels, raising a risk of fluorosis, although exact historical intake levels are difficult to assess.

Conclusion

This study applies an innovative multidisciplinary approach, using new methods to examine skeletal fluorosis in cremated human remains. To the best of the authors' knowledge, it is the first to address this issue from a population perspective and thus contributes to the development of historical ecotoxicology. Although cremated remains raise many difficulties for bioarchaeological studies, the correlation observed between palaeopathological macro-observations and LIBS measurements demonstrates the potential for providing greater scientific certainty in diagnosing pathological conditions such as fluorosis. Further research with a bigger sample, including a larger sample from Cumae and other sites in volcanic regions such as Pompeii, should enable us to enrich and reinforce our results and assess differences between various environments.

For this study, we examined only femur fragments, but to conduct a more comprehensive assessment of intoxication stages, future research should involve analysing other bones (*e.g.* ribs) in order to evaluate fluoride levels in bones with varying turnover rates.

Supplementary information

The supplementary information is available in .pdf from the BMSAP website (https://journals.openedition.org/bmsap/15711?file=1).

Acknowledgments

This research was conducted as part of a PhD funded by the French Ministry of Higher Education and Research, through the *Réseau des Écoles Françaises à l'étranger,* in collaboration with the *École française de Rome*. It also benefited from the scientific framework provided by the University of Bordeaux's IdEx "Investments for the Future" program/GPR "Human Past". The authors are grateful for their collaboration to Professor Jean-Pierre Brun (Collège de France) and to the entire team involved in the "*Cumes : Aux marges de la ville*" research programme. Sincere thanks also to Anne Le Maître, editor-in-chief of the BMSAP, and the anonymous reviewers for their invaluable feedback and constructive comments, which have significantly enhanced the quality of this manuscript.

References

Adinolfi R (1978) I Campi Flegrei nell'antichità (Pozzuoli e Cuma) (vol. I). Azienda autonoma di cura, soggiorno e turismo di Pozzuoli, Napoli, 52 p

Álvarez C, Pisonero J, Bordel N (2014) Quantification of fluorite mass-content in powdered ores using a Laser-Induced Breakdown Spectroscopy method based on the detection of minor elements and CaF molecular bands. Spectrochimica Acta Part B: Atomic Spectroscopy 100:123-128 [https://doi.org/10.1016/j.sab.2014.07.024]

Alvarez-Llamas C, Pisonero J, Bordel N (2016) Quantification of fluorine traces in solid samples using CaF molecular emission bands in atmospheric air Laser-Induced Breakdown Spectroscopy. Spectrochimica Acta Part B: Atomic Spectroscopy 123: 157-162 [https://doi.org/10.1016/j.sab.2016.08.006]

Alvarez-Llamas C, Pisonero J, Bordel N (2017) A novel approach for quantitative LIBS fluorine analysis using CaF emission in calcium-free samples. Journal of Analytical Atomic Spectrometry 32(1):162-166 [https://doi.org/10.1039/C6JA00386A]

Ayoob S, Gupta AK (2006) Fluoride in drinking water: A review on the status and stress effects. Critical Reviews in Environmental Science and Technology 36(6):433-487 [https://doi.org/10.1080/10643380600678112]

Barbier O, Arreola-Mendoza L, Del Razo LM (2010) Molecular mechanisms of fluoride toxicity. Chemico-Biological Interactions 188(2):319-333 [https://doi.org/10.1016/j.cbi.2010.07.011]

Baxter PJ, Horwell CJ (2015) Impacts of eruptions on human health. In: Sigurdsson H (ed) The Encyclopedia of Volcanoes. Academic Press, London, pp 1035-1047 [https://doi.org/10.1016/B978-0-12-385938-9.00060-2]

Benjelloun Y, Carlut J, Hélie J-F et al (2019) Geochemical study of carbonate concretions from the aqueduct of Nîmes (southern France): a climatic record for the first centuries AD? Scientific Reports 9(1):5209 [https://doi.org/10.1038/s41598-019-41620-4]

Boivin G, Chavassieux P, Chapuy MC et al (1989) Skeletal fluorosis: Histomorphometric analysis of bone changes and bone fluoride content in 29 patients. Bone 10(2):89-99 [https://doi.org/10.1016/8756-3282(89)90004-5]

Boskey AL (2007) Mineralization of bones and teeth. Elements 3 (6):385-391 [https://doi.org/10.2113/GSELEMENTS.3.6.385]

Bousquet J-C (2018) Volcans, séismes et tsunamis en Méditerranée. Biotope Éditions, Mèze, 359 p

Brickley M, Ives R (2008a) Miscellaneous conditions. In: Brickley M, Ives R (eds) The Bioarchaeology of Metabolic Bone Disease. Academic Press, San Diego, pp 241-260

Brickley M, Ives R (2008b) The Bioarchaeology of Metabolic Bone Disease (1st ed). Academic Press, San Diego, 350 p

Brun J-P, Gasparri C (2009) Curiosa storia di un labrum cumano. In: Cuma. Indagini Archeologiche e Nuove Scoperte. Studi Cumani 2 (vol. 1). Naus Editoria, Pozzuoli, pp 259-270

Brun J-P, Munzi P (2009) La Necropoli monumentale di età romana a nord della città di Cuma. In: Cuma, Atti del XLVIII Convegno di Studi sulla Magna Grecia. Istituto per la storia e l'archeologia della magna grecia, Taranto, pp 635-717 [https://hal.science/hal-01673906]

Brun J-P, Munzi P, Cavassa L et al (2013) Cumes. Chronique des activités archéologiques de l'École française de Rome, Italie du Sud [https://doi.org/10.4000/cefr.989]

Brun J-P, Munzi P, Girardot S et al (2010) Un mausoleo a tumulo di età tardo-repubblicana nella necropoli settentrionale di Cuma. In: Gasparri C, Greco G, Pierobon R (eds) Dall'immagine Alla Storia. Studi per Ricordare Stefania Adamo Muscettola 10, Naus Editoria, Pozzuoli, pp 279-302 [https://hal.science/hal-01435853]

Bruzek J (2002) A method for visual determination of sex, using the human hip bone. American Journal of Physical Anthropology 117(2):157-168 [https://doi.org/10.1002/ajpa.10012]

Buchancová J, Poláček H, Hudečková H et al (2008) Skeletal fluorosis from the point of view of an occupational exposure to fluorides in former Czechoslovakia. Interdisciplinary Toxicology 1(2):193-197 [https://doi.org/10.2478/v10102-010-0038-7]

Callaghan RT (1986) Analysis of the fluoride content of human remains from the Gray site, Saskatchewan. Plains Anthropologist 31(114):317-328 [https://doi.org/10.1080/2052546.1986.11909347]

Calò M, Tramelli A (2018) Anatomy of the Campi Flegrei caldera using Enhanced Seismic Tomography Models. Scientific Reports 8(1):16254 [https://doi.org/10.1038/s41598-018-34456-x]

Camodeca G (1997) Una ignorata galleria stradale d'età augustea fra Lucrinum e Baiae e la più antica iscrizione di un curator aquae Augustae (10 d.C.). Annali Di Archeologia e Storia Antica 4:191-199

Capaldi C (2007a) Lo scavo del settore sud-orientale del Foro. In: Gasparri C, Greco G (eds) Cuma. Il Foro. Scavi Dell'Università Di Napoli Federico II 2000-2001. Atti Della Giornata Di Studi, Napoli 22 Giugno 2002. Naus Editoria, Pozzuoli, pp 137-162

Capaldi C (2007b) Nuove attestazioni epigrafiche della gens Lucceia. In: Gasparri C, Greco G (eds) Cuma. Il Foro. Scavi Dell'Università Di Napoli Federico II 2000-2001. Atti Della Giornata Di Studi, Napoli 22 Giugno 2002. Naus Editoria, Pozzuoli, pp 163-176

Capaldi C (2008) Il ninfeo e la fontana dei Luccei. In: Zevi F, Demma F, Nuzzo E (eds) Museo Archeologico Dei Campi Flegrei. Catalogo Generale. Cuma (vol. 1). Electa, Napoli, pp 314-315

Cappelletti P, Fedele L, Petrosino P et al (2022) Geologia ed archeologia nei Campi Flegrei:un incontro virtuoso. In: De Bonis A, Pagano F, Del Villano M (eds) Terra: la scultura di un paesaggio. Gangemi editore SpA international, Roma, pp 37-46

Caputo P (2004) La Grotta di Cocceio a Cuma: nuovi dati da ricerche e saggi di scavo. Atlante Tematico Di Topografia Antica 13:309-330

Caputo P, Morichi R, Paone R et al (1996) Cuma e il suo parco archeologico. Un territorio e le sue testimonianze. Scienze e Lettere, Roma, 222 p

Carlut J, Chazot G, Dessales H et al (2009) Trace element variations in an archeological carbonate deposit from the antique city of Ostia: Environmental and archeological implications. Comptes Rendus Geoscience 341(1):10-20 [https://doi.org/10.1016/j.crte.2008.09.006]

Chowdhury A, Adak MK, Mukherjee A et al (2019) A critical review on geochemical and geological aspects of fluoride belts, fluorosis and natural materials and other sources for alternatives to fluoride exposure. Journal of Hydrology 574: 333-359 [https://doi.org/10.1016/j.jhydrol.2019.04.033]

Ciaramella A, De Lauro E, Falanga M et al (2011) Automatic detection of long-period events at Campi Flegrei Caldera (Italy): Seismicity analysis at Campi Flegrei. Geophysical Research Letters 38(L18302):1-5 [https://doi.org/10.1029/2011GL049065]

Cook FJ, Seagrove-Guffey M, Mumm S et al (2021) Non-endemic skeletal fluorosis: Causes and associated secondary hyperparathyroidism (case report and literature review). Bone 145:115839 [https://doi.org/10.1016/j.bone.2021.115839]

D'Acunto M (2020) Cuma: i sistemi di regimentazione delle acque di epoca arcaica, la pianificazione urbana e la tirannide di Aristodemo. In: Opere Di Regimentazione Delle Acque in Età Arcaica. Roma, Grecia e Magna Grecia, Etruria e Mondo Italico. Quasar Editions, Paris, pp 255-324

D'Alessandro W (2006) Human fluorosis related to volcanic activity: a review. In: Kungolos AG, Brebbia CA, Samaras CP et al (eds) Environmental Toxicology (vol. 10). Mykonos, Greece: WIT Press, p. 21-30 [https://doi:10.2495/ETOX060031]

Datta P, Datta PP (2013) Prevalence, etiology and clinical features of skeletal fluorosis: a critical review. Innovare Journal of Medical Sciences 1:5-6

de Vlam K, Lories RJ, Luyten FP (2006) Mechanisms of pathologic new bone formation. Current Rheumatology Reports 8 (5):332-337 [https://doi.org/10.1007/s11926-006-0061-z]

Delile H (2014) Signatures des paléo-pollutions et des paléo-environnements dans les archives sédimentaires des ports antiques de Rome et d'Éphèse. Thèse de doctorat, Université Lumière Lyon 2, Lyon

Depierre G (2014) Crémation et archéologie : nouvelles alternatives méthodologiques en ostéologie humaine. Éditions universitaires de Dijon, Dijon, 654 p

Dessales H (2008) Des usages de l'eau aux évaluations démographiques : l'exemple de Pompéi. Histoire urbaine 22(2):27-41 [https://doi.org/10.3917/rhu.022.0027]

Dessales H (2013) Le partage de l'eau. Fontaines et distribution hydraulique dans l'habitat urbain de l'Italie romaine. École française de Rome, Rome, 602 p

Di Vito MA, Isaia R, Orsi G et al (1999) Volcanism and deformation since 12,000 years at the Campi Flegrei caldera (Italy). Journal of Volcanology and Geothermal Research 91(2):221-246 [https://doi.org/10.1016/S0377-0273(99)00037-2]

Döring M (2012) In der wundersamsten Gegend der Welt: die Phlegraeischen Felder am Golf von Neapel. Parmenios, Adenstedt, 306 p

Ducci D, Sellerino M (2012) Natural background levels for some ions in groundwater of the Campania region (southern Italy). Environmental Earth Sciences 67(3):683-693 [https://doi.org/10.1007/s12665-011-1516-8]

Duday H (2009) The Archaeology of the Dead: Lectures in Archaeothanatology. Oxbow Books, Oxford/Oakville, 158 p

Duday H (2018) Les restes humains et la définition de la tombe à l'époque romaine. L'apport des liaisons ostéologiques dans l'étude des sépultures secondaires à crémation à partir d'exemples de Pompéi, Rome, Ravenne et Cumes. In : Nenna M-D, Huber S, Van Andringa W (eds) Constituer la tombe, honorer les défunts en Méditerranée antique. Centre d'études alexandrines, Alexandrie, pp 403-429

Duday H (2019) Sépultures secondaires à crémation : quelques réflexions sur trente années d'évolution méthodologique en France. Les Nouvelles de l'Archéologie 157-158:100-106 [https://doi.org/10.4000/nda.7831]

Duday H, Depierre G, Janin T (2000) Validation des paramètres de quantification, protocoles et stratégies dans l'étude anthropologique des sépultures secondaires à incinération. L'exemple des nécropoles protohistoriques du Midi de la France. In : Archéologie de la tombe au premier âge du Fer, Monographie d'Archéologie Méditerranéenne 5, Lattes, pp 7-29

Eager JM (1901) Denti di Chiaie (Chiaie teeth). Public Health Reports (1896-1970) 16:2576-2577

Emslie SD, Brasso R, Patterson WP et al (2015) Chronic mercury exposure in Late Neolithic/Chalcolithic populations in Portugal from the cultural use of cinnabar. Scientific Reports 5(1): 14679 [https://doi.org/10.1038/srep14679]

Fabreau GE, Bauman P, Coakley AL et al (2019) Skeletal fluorosis in a resettled refugee from Kakuma refugee camp. The Lancet 393(10168):223-225 [https://doi.org/10.1016/S0140-6736(18)32842-3]

Ferrari G, Lamagna R (2013) The Augustean aqueduct in the Phlegraean Fields (Naples, Southern Italy). 16th International Congress of Speleology, Brno, vol. 2, pp 200-205

Ferrari G, Lamagna R (2016) L'acquedotto auguesteo della Campania nei Campi Flegrei (Napoli). Archeologia Sotterranea 16:24-33

Ferrari G, Lamagna R, Rognoni E (2018) Aqua Augusta: nuove evidenze dai Campi Flegrei. Atti delle Giornate di Studio "Evidenze archeologiche e profili giuridici della rete idrica in Campania", Napoli, pp 37-94

Forni F, Degruyter W, Bachmann O et al (2018) Long-term magmatic evolution reveals the beginning of a new caldera cycle at Campi Flegrei. Science Advances 4(11):eaat9401 [https://doi.org/10.1126/sciadv.aat9401]

Foucaud Y, Fabre C, Demeusy B et al (2019) Optimisation of fast quantification of fluorine content using handheld laser induced breakdown spectroscopy. Spectrochimica Acta Part B: Atomic Spectroscopy 158:105628 [https://doi.org/10.1016/j.sab.2019.05.017]

Fresnais M, Richardin P, Gimat A et al (2015) Recent advances in the characterization of hair of mummies from the Chilean Andean coast. Forensic Science International 249:25-34 [https://doi.org/10.1016/j.forsciint.2015.01.005]

Gaft M, Nagli L, Eliezer N et al (2014) Elemental analysis of halogens using molecular emission by laser-induced breakdown spectroscopy in air. Spectrochimica Acta Part B: Atomic Spectroscopy 98:39-47 [https://doi.org/10.1016/j.sab.2014.05.011]

Galaz-Mandakovic D, Rivera F (2022) Copper sulfide mining at Chuquicamata and the spread of arsenic in drinking water in Chile, 1952-1971: A derivation of extractivism. The Extractive Industries and Society 11:101135 [https://doi.org/10.1016/j.exis.2022.101135]

Gallo A (2015) Una 'fistula Aquaria' Della 'Res Publica Cumanorum' a San Marino. ACME: Annali Della Facoltà Di Lettere e Filosofia Dell'Università Degli Studi Di Milano 68(1):97-128 [https://doi.org/10.13130/2282-0035/5138]

Gasparri C (2009) Il Foro di Cuma dal I sec. a. C. all'età bizantina. In: Cuma. Atti Del Quarantottesimo Convegno Di Studi Sulla Magna Grecia (vol. 1). Scorpione editrice srl, Taranto, pp 579-611

Ghosh A, Mukherjee K, Ghosh SK et al (2013) Sources and toxicity of fluoride in the environment. Research on Chemical Intermediates 39(7):2881-2915 [https://doi.org/10.1007/s11164-012-0841-1]

Guan Z, Wang L, Sun D (2019) Endemic Fluorosis. In: Sun D (ed) Endemic Disease in China (vol. 2). Springer Singapore, Singapore, pp 61-96 [https://doi.org/10.1007/978-981-13-2529-8_3]

Guardascione FM (2007) Le terme del Foro e un inedito castellum aquae secondario della città bassa di Cuma. Cuma. Indagini Archeologiche e Nuove Scoperte, Atti Della Giornata Di Studi, Napoli 12:309-318

Gupta AK, Ayoob S (2016) Skeletal fluorosis. In: Gupta AK, Ayoob S (eds) Fluoride in Drinking Water. Status, Issues, and Solutions. CRC Press, Boca Raton, pp 39-50

Gutherz X (1986) Informations archéologiques : circonscription de Languedoc-Roussillon. Gallia Préhistoire 29(2):353-380

Izuora K, Twombly JG, Whitford GM et al (2011) Skeletal Fluorosis from Brewed Tea. The Journal of Clinical Endocrinology & Metabolism 96(8):2318-2324 [https://doi.org/10.1210/jc.2010-2891]

Jantzi SC, Motto-Ros V, Trichard F et al (2016) Sample treatment and preparation for laser-induced breakdown spectroscopy. Spectrochimica Acta Part B: Atomic Spectroscopy 115:52-63 [https://doi.org/10.1016/j.sab.2015.11.002]

Jolly SS, Singh BM, Mathur OC et al (1968) Epidemiological, clinical, and biochemical study of endemic dental and skeletal fluorosis in Punjab. British Medical Journal 4(5628):427-429 [https://doi.org/10.1136/bmj.4.5628.427]

Joseph A, Rajan R, Paul J et al (2022) The continuing crippling challenge of skeletal fluorosis – Case series and review of literature. Journal of Clinical and Translational Endocrinology: Case Reports 24:100114 [https://doi.org/10.1016/j.jecr.2022.100114]

Keenan-Jones D (2010a) The Aqua Augusta and control of water resources in the Bay of Naples. Proceeding of the Australasian Society for Classical Studies Conference, Perth 31:1-18

Keenan-Jones D (2010b) The Aqua Augusta: Regional Water Supply in Roman and Late Antique Campania. PhD Thesis, Macquarie University, Sydney

Keenan-Jones D (2013) Large-scale water management projects in Roman central-southern Italy. In: Harris W (ed) The Ancient Mediterranean Environment between Science and History. Columbia Studies in the Classical Tradition 39, Brill, Leyde, pp 233-256 [https://doi.org/10.1163/9789004254053_011]

Khairnar MR, Dodamani AS, Jadhay HC et al (2015) Mitigation of Fluorosis - A Review. Journal of Clinical and Diagnostic Reseach9(6):5-9[https://doi.org/10.7860/JCDR/2015/13261.6085]

Kurdi M (2016) Chronic fluorosis: The disease and its anaesthetic implications. Indian Journal of Anaesthesia 60(3):157 [https://doi.org/10.4103/0019-5049.177867]

Lerebours C, Weinkamer R, Roschger A et al (2020) Mineral density differences between femoral cortical bone and trabecular bone are not explained by turnover rate alone. Bone Reports 13:100731 [https://doi.org/10.1016/j.bonr.2020.100731]

Linoli A (2012) L'Aqua Augusta. Un sistema acquedottistico del I secolo a.C. al servizio del Golfo di Napoli. L'Acqua 5:29-44

Littleton J (1999) Paleopathology of skeletal fluorosis. American Journal of Physical Anthropology 109(4):465-483 [https://doi.org/10.1002/(SICI)1096-8644(199908)109:4<465::AID-AJPA4>3.0.CO;2-T]

Loeff A (2018) Le diagnostic de fluorose à partir de restes humains brûlés L'intoxication de la population romaine de Cumes par les eaux de boisson. Mémoire de Master 2, Université de Bordeaux, Pessac

Mays LW, Koutsoyiannis D, Angelakis AN (2007) A brief history of urban water supply in antiquity. Water Supply 7(1):1-12 [https://doi.org/10.2166/ws.2007.001]

McKinley JI (1993) Bone fragment size and weights of bone from modern British cremations and the implications for the interpretation of archaeological cremations. International Journal of Osteoarchaeology 3(4):283-287 [https://doi/10.1002/oa.1390030406]

Meindl RS, Lovejoy CO (1989) Age changes in the pelvis: implications for paleodemography. In: Yaşar İşcan M. (ed) Age Markers in the Human Skeleton. Charles C. Thomas publisher, Springfield, pp 137-168

Miller RF, Phillips PH (1953) The metabolism of fluorine in the bones of the fluoride-poisoned rat. The Journal of Nutrition 51(2):273-281 [https://doi.org/10.1093/jn/51.2.273]

Miller RF, Phillips PH (1956) The effect of age on the level and metabolism of fluorine in the bones of the fluoridated rat. The Journal of Nutrition 59(3):425-433 [https://doi.org/10.1093/jn/59.3.425]

Mohammadi AA, Yousefi M, Yaseri M et al (2017) Skeletal fluorosis in relation to drinking water in rural areas of West Azerbaijan, Iran. Scientific Reports 7(1):17300:1-7 [https://doi.org/10.1038/s41598-017-17328-8]

Moore J (2019) Death Metal: Characterising the effects of environmental lead pollution on mobility and childhood health within the Roman Empire. PhD Thesis, Durham University, Durham [http://etheses.dur.ac.uk/13292/]

Moore J, Filipek K, Kalenderian V et al (2021) Death metal: Evidence for the impact of lead poisoning on childhood health within the Roman Empire. International Journal of Osteoarchaeology 31(5):846-856 [https://doi.org/10.1002/oa.3001]

Munzi P (2022) Morire a Cuma. La necropoli della Porta mediana delle fortificazioni settentrionali. In: Pagano F, Del Villano M (eds) Terra: la scultura di un paesaggio. Gangemi Editore, Roma, pp 185-239

Munzi P, Brun J-P (2011) Cumes (Italie). Les fouilles du Centre Jean-Bérard 2000-2010. Bulletin de la Société française d'Archéologie classique 51(1):147

Munzi P, Brun J-P, Duday H et al (2018) "All'ombra de'cipressi e dentro le urne...". La latinizzazione della necropoli cumana. Antropologie e Archeologie a Confronto, RomArché, Roma, pp 313-341 [https://hal.science/hal-01677539]

Nelson EA (2015) Possible fluoride toxicity in North America: A paleopathological assessment and discussion of modern occurrence. MSc thesis, University of North Texas, Denton

Nelson EA, Halling CL, Buikstra JE (2016) Investigating fluoride toxicity in a Middle Woodland population from west-central Illinois: A discussion of methods for evaluating the influence of environment and diet in paleopathological analyses. Journal of Archaeological Science: Reports 5:664-671 [https://doi.org/10.1016/j.jasrep.2016.01.004]

Nelson EA, Halling CL, Buikstra JE (2019) Evidence of skeletal fluorosis at the Ray site, Illinois, USA: A pathological assessment and discussion of environmental factors. International Journal of Paleopathology 26:48-60 [https://doi.org/10.1016/j.ijpp.2019.05.003]

Orsi G, Civetta L, Del Gaudio C et al (1999) Short-term ground deformations and seismicity in the resurgent Campi Flegrei caldera (Italy): An example of active block-resurgence in a densely populated area. Journal of Volcanology and Geothermal Research 91(2-4):415-451 [https://doi.org/10.1016/S0377-0273(99)00050-5]

Ortner DJ (2003) Identification of Pathological Conditions in Human Skeletal Remains (2nd ed). Academic Press, San Diego, 664 p

Özdemir K, Erdal YS, Demirci Ş (2010) Arsenic accumulation on the bones in the Early Bronze Age İkiztepe population, Turkey. Journal of Archaeological Science 37(5):1033-1041 [https://doi.org/10.1016/j.jas.2009.12.004]

Ozsvath DL (2009) Fluoride and environmental health: a review. Reviews in Environmental Science and Bio/Technology 8(1): 59-79 [https://doi.org/10.1007/s11157-008-9136-9]

Parfitt AM (2002) Misconceptions (2): Turnover is always higher in cancellous than in cortical bone. Bone 30(6):807-809 [https://doi.org/10.1016/S8756-3282(02)00735-4]

Petrone P, Giordano M, Giustino S et al (2011) Enduring fluoride health hazard for the Vesuvius area population: The case of AD 79 Herculaneum. PLoS ONE 6(6):e21085 [https://doi.org/10.1371/journal.pone.0021085]

Petrone P, Graziano V, Sastri C et al (2019) Dental fluorosis in the Vesuvius towns in AD 79: A multidisciplinary approach. Annals of Human Biology 46(5):388-392 [https://doi.org/10.1080/03014460.2019.1640791]

Petrone P, Guarino FM, Giustino S et al (2013) Ancient and recent evidence of endemic fluorosis in the Naples area. Journal of Geochemical Exploration 131:14-27 [https://doi.org/10.1016/j.gexplo.2012.11.012]

Ponikvar M (2008) Exposure of humans to fluorine and its assessment. In: Tressauad A, Haufe G (eds) Fluorine and Health: Molecular Imaging, Biomedical Materials and Pharmaceuticals. Elsevier, Amsterdam, pp 487-549 [https://doi.org/10.1016/B978-0-444-53086-8.00012-6]

Pořízka P, Kaski S, Hrdlička A et al (2017) Detection of fluorine using laser-induced breakdown spectroscopy and Raman spectroscopy. Journal of Analytical Atomic Spectrometry 32 (10):1966-1974 [https://doi.org/10.1039/C7JA00200A]

Potenza U (2016) L'acqua di Serino e l'acquedotto Augusteo. L'Acquaonline 7

Proctor TK (2021) Mercury, Mitayos, and the Violence of the Everyday: The Bioarchaeology of the Santa Bárbara Mercury Mines in Huancavelica, Peru (16th-19th Centuries CE). PhD thesis, Vanderbilt University, Vanderbilt

Qin X, Wang S, Yu M et al (2009) Child skeletal fluorosis from indoor burning of coal in southwestern China. Journal of Environmental and Public Health 2009:1-7 [https://doi.org/10.1155/2009/969764]

Rehse SJ, Salimnia H, Miziolek AW (2012) Laser-induced breakdown spectroscopy (LIBS): an overview of recent progress and future potential for biomedical applications. Journal of Medical Engineering & Technology 36(2):77-89 [https://doi.org/10.3109/03091902.2011.645946]

Rho J-Y, Kuhn-Spearing L, Zioupos P (1998) Mechanical properties and the hierarchical structure of bone. Medical Engineering & Physics 20(2):92-102 [https://doi.org/10.1016/S1350-4533(98)00007-1]

Rosi M, Sbrana A, Principe C (1983) The Phlegraean Fields: Structural evolution, volcanic history and eruptive mechanisms. Journal of Volcanology and Geothermal Research 17(1-4): 273-288 [https://doi.org/10.1016/0377-0273(83)90072-0]

Sahu P (2019) Fluoride pollution in groundwater. In: Sikdar PK (ed) Groundwater Development and Management. Springer International Publishing, Cham, pp 329-350 [https://doi.org/10.1007/978-3-319-75115-3_14]

Samek O, Beddows DCS, Telle HH et al (2001) Quantitative laser-induced breakdown spectroscopy analysis of calcified tissue samples. Atomic Spectroscopy 11 [https://doi.org/10.1016/S0584-8547(01)00198-7]

Sánchez-Bayo F (2011) Sources and toxicity of pollutants. In: Sánchez-Bayo F, van den Brink P, Mann R (eds) Ecological Impacts of Toxic Chemicals. Bentham Science Publishers, Sharjah, pp 3-12

Sbrana A, Marianelli P, Pasquini G (2021) The Phlegrean Fields volcanological evolution. Journal of Maps 17(2):557-570 [https://doi.org/10.1080/17445647.2021.1982033]

Scheid J (ed) (2008) Pour une archéologie du rite : nouvelles perspectives de l'archéologie funéraire. École française de Rome, Rome, 358 p

Scheuer L, Black S (2000) Development and ageing of the juvenile skeleton. In: Cox M, Mays S (eds) Human Osteology in Archaeology and Forensic Science. Cambridge University Press, New York, pp 9-22

Sellami M, Riahi H, Maatallah K et al (2020) Skeletal fluorosis: Don't miss the diagnosis! Skeletal Radiology 49(3):345-357 [https://doi.org/10.1007/s00256-019-03302-0]

Shaji E, Sarath KV, Santosh M et al (2024) Fluoride contamination in groundwater: A global review of the status, processes, challenges, and remedial measures. Geoscience Frontiers 15 (2):101734 [https://doi.org/10.1016/j.gsf.2023.101734]

Shamsollahi HR, Zolghadr Z, Mahvi AH et al (2015) The effect of temperature, water hardness, and exposure time on fluoride toxicity in the aquatic environment. Fluoride 48(4):338

Spizzichino V, Fantoni R (2014) Laser Induced Breakdown Spectroscopy in archeometry: A review of its application and future perspectives. Spectrochimica Acta Part B: Atomic Spectroscopy 99:201-209 [https://doi.org/10.1016/j.sab.2014.07.003]

Srivastava S, Flora SJS (2020) Fluoride in drinking water and skeletal fluorosis: A review of the global impact. Current Environmental Health Reports 7(2):140-146 [https://doi.org/10.1007/s40572-020-00270-9]

Stellato L, Coda S, Arienzo M et al (2020) Natural and anthropogenic groundwater contamination in a coastal volcanic-sedimentary aquifer: The case of the archaeological site of Cumae (Phlegraean Fields, Southern Italy). Water 12(12):3463 [https://doi.org/10.3390/w12123463]

Syvilay D, Bousquet B, Chapoulie R et al (2019) Advanced statistical analysis of LIBS spectra for the sourcing of obsidian samples. Journal of Analytical Atomic Spectrometry 34(5): 867-873[https://doi.org/110.1039/C8JA00340H]

Talal A, Hamid SK, Khan M et al (2020) Structure of biological apatite: Bone and tooth. In: Khan AS, Chaudhry AA (eds) Handbook of Ionic Substituted Hydroxyapatites. Woodhead Publishing, Duxford, pp 1-19 [https://doi.org/10.1016/B978-0-08-102834-6.00001-X]

Teotia M, Teotia SPS, Kunwar KB (1971) Endemic skeletal fluorosis. Archives of Disease in Childhood 46(249):686-691 [https://doi.org/10.1136/adc.46.249.686]

Teotia SPS, Teotia M (1988) Endemic skeletal fluorosis: clinical and radiological variants. Fluoride 21(1):39-44

Teotia SPS, Teotia M, Singh DP (1986) Bone static and dynamic histomorphometry in endemic skeletal fluorosis. In: Studies in Environmental Science (vol. 27). Elsevier, Amsterdam, pp 347-355 [https://doi.org/10.1016/S0166-1116(08)71861-2]

Tölle-Kastenbein R (1993) Archeologia dell'acqua: la cultura idraulica nel mondo classico. Longanesi, Milano, 275 p

Torino M, Naji S, Munzi P et al (2012) Dental fluorosis in ancient Cuma, Italy. American Journal of Physical Anthropology 147(S54):287

Torino M, Rognini M, Fornaciari G (1995) Dental fluorosis in ancient Herculaneum. The Lancet 345(8960):1306 [https://doi.org/10.1016/S0140-6736(95)90952-4]

Turkekul R, Arihan SK, Yildirim S et al (2020) Effect of acute and chronic fluoride administration on bone histopathology, bone fluoride accumulation, and locomotor activity in an animal model of paleopathological fluorosis. Fluoride 53(1):77-89

Van Andringa W, Duday H, Lepetz S et al (2013) Mourir à Pompéi : fouille d'un quartier funéraire de la nécropole romaine de Porta Nocera ; 2003-2007 (vols 1-2). École française de Rome, Rome, 1541 p

Van Andringa W, Duday H, Boisson A et al (2021) Pompéi Porta Nocera – Campagne 2021. Rapport final d'opération programmée [https://hal.science/hal-03964415]

Villotte S, Assis S, Cardoso FA et al (2016) In search of consensus: Terminology for entheseal changes (EC). International Journal of Paleopathology 13:49-55 [https://doi.org/10.1016/j.ijpp.2016.01.003]

Villotte S, Castex D, Couallier V et al (2010) Enthesopathies as occupational stress markers: evidence from the upper limb. American Journal of Physical Anthropology 142(2):224-234 [https://doi.org/10.1002/ajpa.21217]

Villotte S, Knüsel CJ (2013) Understanding entheseal changes: definition and life course changes. International Journal of Osteoarchaeology 23(2):135-146 [https://doi.org/10.1002/oa.2289]

Walser JW, Gowland RL, Desnica N et al (2020) Hidden dangers? Investigating the impact of volcanic eruptions and skeletal fluorosis in medieval Iceland. Archaeological and Anthropological Sciences 12(3):1-23 [https://doi.org/10.1007/s12520-020-01026-0]

Wei W, Pang S, Sun D (2019) The pathogenesis of endemic fluorosis: Research progress in the last 5 years. Journal of Cellular and Molecular Medicine 23(4):2333-2342 [https://doi.org/10.1111/jcmm.14185]

Weinstein P (2005) Palaeopathology by proxy: The case of Egil's bones. Journal of Archaeological Science 32(7):1077-1082 [https://doi.org/10.1016/j.jas.2005.02.008]

Whitford GM (1994) Intake and metabolism of fluoride. Advances in Dental Research 8(1):5-14 [https://doi.org/10.1177/08959374940080011001]

Whitford GM (1999) Fluoride Metabolism and Excretion in Children. Journal of Public Health Dentistry 59(4):224-228 [https://doi.org/10.1111/j.1752-7325.1999.tb03273.x]

WHO (1984) Fluorine and fluorides. World Health Organization, Geneva, 136 p [https://iris.who.int/handle/10665/37288]

WHO (1992) Endemic fluorosis: a global health issue, a technical report for the Human Exposure Assessment Locations Project. In: Endemic Fluorosis: A Global Health Issue. A Technical Report for the Human Exposure Assessment Locations Project. World Health Organization, Geneva, p 58 [https://iris.who.int/handle/10665/59588]

WHO (2019) Preventing disease through healthy environments: inadequate or excess fluoride: a major public health concern. World Health Organization, Geneva, 8 p [https://www.who.int/publications/i/item/9789241565196]

Yeşilnacar Mİ, Demir Yetiş A, Dülgergil ÇT et al (2016) Geomedical assessment of an area having high-fluoride groundwater in southeastern Turkey. Environmental Earth Sciences 75(2): 162 [https://doi.org/10.1007/s12665-015-5002-6]

Yildiz M, Oral B (2003) Effects of menopause on bone mineral density in women with endemic fluorosis. Clinical Nuclear Medicine 28(4):308-311 [https://doi.org/10.1097/01.RLU.0000057557.56231.EE]

Yoshimura K, Nakahashi T, Saito K (2006) Why did the ancient inhabitants of Palmyra suffer fluorosis? Journal of Archaeological Science 33(10):1411-1418 [https://doi.org/10.1016/j.jas.2006.01.016]

Zevi F, Demma F, Nuzzo E (2008) Museo archeologico dei Campi Flegrei: catalogo generale. Electa Napoli, Cuma, 448 p

Zhou Y, Liu K, Yan F et al (2023) Two cases of skeletal fluorosis from the historic cemetery at Zhangwan, Henan Province, China. International Journal of Osteoarchaeology oa.3266 [https://doi.org/10.1002/oa.3266]

Zohoori FV, Duckworth RM (2017) Fluoride. In: Collins JF (ed) Molecular, Genetic, and Nutritional Aspects of Major and Trace Minerals. Elsevier, Amsterdam, pp 539-550 [https://doi.org/10.1016/B978-0-12-802168-2.00044-0]

Zuo H, Chen L, Kong M et al. (2018) Toxic effects of fluoride on organisms. Life Sciences 198:18-24 [https://doi.org/10.1016/j.lfs.2018.02.00]